

Aromatic Molecular-Bowl Hydrocarbons: Synthetic Derivatives, Their Structures, and Physical Properties

Yao-Ting Wu*[†] and Jay S. Siegel*[‡]

Department of Chemistry, National Cheng-Kung University, No. 1 Ta-Hsueh Road, Tainan, Taiwan and Institute of Organic Chemistry, University of Zurich, Winterthurerstrasse 190, CH-8057 Zurich, Switzerland

Received June 9, 2006

Contents

1. Introduction	4843
2. Corannulene and Its Derivatives	4843
2.1. Corannulene	4843
2.1.1. Pioneering Syntheses	4843
2.1.2. Structure and Properties	4847
2.2. Highly Substituted Corannulenes	4850
2.2.1. Synthesis	4850
2.2.2. Structures and Properties	4851
2.3. Cyclopentacorannulene, Acecorannulene, and <i>peri</i> -Annulated Corannulenes	4852
2.3.1. Synthesis	4852
2.3.2. Structures and Properties	4852
2.4. Dibenzocorannulenes	4854
2.4.1. Synthesis	4854
2.4.2. Structures and Properties	4855
2.5. Indenocorannulenes	4855
2.5.1. Synthesis	4855
2.5.2. Structures and Properties	4855
2.6. Other Corannulene Derivatives	4855
2.7. Complexed Corannulenes and Their Derivatives	4857
2.7.1. η^6 -Complexed Corannulenes and Their Derivatives	4857
2.7.2. η^2 -Complexed Corannulenes and Their Derivatives	4861
2.7.3. Metal-Bonded Derivatives of Corannulene	4863
2.7.4. η^n -Complexed Corannulenes and Their Derivatives in the Gas Phase	4863
2.8. Correlations between Structures and Bowl-to-Bowl Inversion Energy (ΔG_{inv}^\ddagger)	4864
3. Sumanene	4864
4. Molecular Packing of Bowls in the Solid State	4865
5. Conclusions and Outlook	4865
6. References	4865

1. Introduction

Euler, a Swiss mathematician, demonstrated that a planar sheet of hexagons can be converted to a curved surface by inclusion of pentagons, 12 being a “magic” number for the creation of closed surfaces.¹ In a chemical context, methods for the synthesis of sp^2 carbon sheets with five-membered

rings among networks of six-membered rings allow the synthesis of chemical Eulerian-curved surfaces, like corannulene (dibenzo[*ghi,mno*]fluoranthene, **1**), fullerenes (**2**), and capped carbon tubes **3** (Chart 1).²

Corannulene was first prepared in 1966 and characterized as a bowl-shaped polynuclear aromatic hydrocarbon (PAH).⁶ Less than two decades later, Kroto, Heath, O’Brien, Curl, and Smalley discovered buckminsterfullerene (**2**) in graphite vapors.³ The icosahedral cage structure of **2** consists of 20 six-membered rings and 12 five-membered rings; the five-membered rings (or corannulene fragment) provide the curvature. In 1991, Japanese researchers observed a related class of three-dimensional carbon surfaces, namely, carbon nanotubes **3**.⁴ Single-walled carbon nanotubes (SWNTs) can be regarded as tubular polyhexagons with two Eulerian-curved end caps. The smallest size (diameter) limit for a SWNT has still not been determined. The C_{20} end cap, namely, corannulene (**1**), is a potential candidate for a seeding structure en route to SWNT.⁵

Numerous additional examples of the [5]circulene motif in curved carbon surfaces exist. Indeed, the corannulene skeleton is an elementary subunit of virtually all Eulerian carbon surfaces. In this review, the synthetic methods and physical properties of molecule bowls based on the corannulene motif will be presented.

2. Corannulene and Its Derivatives

2.1. Corannulene

2.1.1. Pioneering Syntheses

Corannulene (**1**) was first synthesized from acenaphthene in 17 steps by Lawton and Barth in 1966.⁶ As mentioned by them: “*Within its structural framework is an unusual strain resulting from the geometrical requirement that the bond angles deviate appreciably from the normal values found for benzenoid compounds.*” Thus, introduction of strain as late as possible was key to their synthetic strategy for the preparation of **1**.⁷

Their synthesis starts with acenaphthalene (**4**) to afford the first key intermediate, 3-carbomethoxy-4*H*-cyclopenta[*def*]phenanthrene (**5**), over five steps using the method of Sieglitz and Schidlo (Scheme 1).⁸ Treatment of **5** with *N*-bromosuccinimide gives bromide **6**, which can be alkylated with triethyl 1,1,2-ethanetricarboxylate in the presence of potassium *tert*-butoxide and *tert*-butyl alcohol and subsequent hydrolysis with aqueous potassium hydroxide to generate diacid diester **7**. Cyclization of **7** with polyphosphoric acid

* To whom correspondence should be addressed. E-mail: jss@oci.unizh.ch.

[†] National Cheng-Kung University.

[‡] University of Zurich.



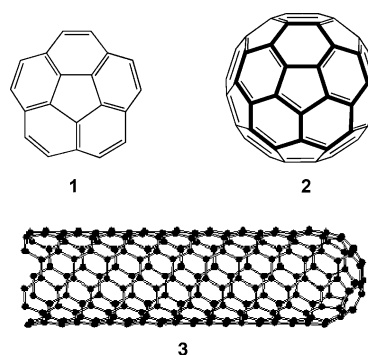
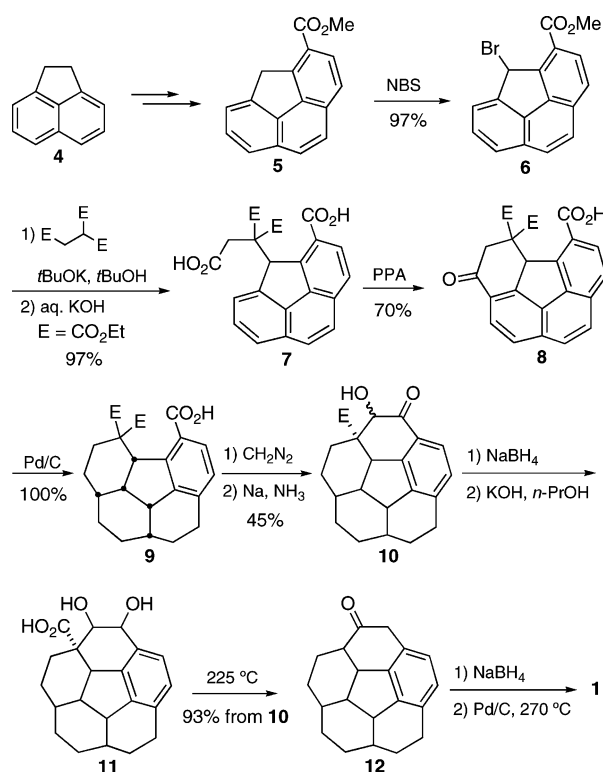
Yao-Ting Wu was born in Taiwan in 1972 and received his B.Sc. degree from National Cheng-Kung University in Taiwan in 1995. After 2 years of military service, he studied chemistry at the University of Göttingen in Germany and obtained his Diplom in 2000 and Dr. rer. nat. in 2003 under the supervision of Professor Armin de Meijere. In 2004, he joined the research group of Professor Jay S. Siegel as a postdoctoral fellow, working on the synthesis of corannulene derivatives and studying their physical properties. He has been Assistant Professor at National Cheng-Kung University in Taiwan since the summer of 2005. His research interests concern organometallic catalysts, polycyclic aromatic compounds, and organic (nano)materials.



Jay S. Siegel was born in California in 1959. He received his B.Sc. degree from California State University, Northridge, in 1980. At Princeton he took up graduate studies in Chemistry with Professor Kurt Martin Mislow and earned his M.S. (1982) and Ph. D. degrees (1985) in the area of Structural Chemistry and Stereochemistry. During his studies at Princeton (1983), he received a Swiss Universities Grant (cf. Fulbright Grants) to spend a year studying crystallography at the Swiss Federal Institute of Technology in Zurich, with Professor Jack. D. Dunitz. After earning his Ph.D. degree he continued his studies in supramolecular chemistry as a NSF-CNRS postdoctoral fellowship with Jean-Marie Lehn at the University of Louis Pasteur in Strasbourg. He began his independent career as Assistant Professor of Chemistry in 1986 at UCSD and was promoted to Associate Professor in 1992 and Full Professor in 1996. He was named a US-NSF Presidential Young Investigator in 1988, an American Cancer Society Jr. Fellow in 1990, an Alfred P. Sloan Fellow in 1992, and an Arthur C. Cope Scholar by the ACS in 1998. He was elected fellow of the American Association for the Advancement of Science in 1998. He has been visiting professor at Princeton, Caltech, University of Basel, the Weizmann Institute, and Tokyo Institute of Technology. In 2003, he was appointed as Professor and Co-director of the Organic Chemistry Institute of the University of Zurich and Director of its laboratory for process chemistry research (LPF). His research interests focus on the synthesis and stereochemistry of designed molecular architectures.

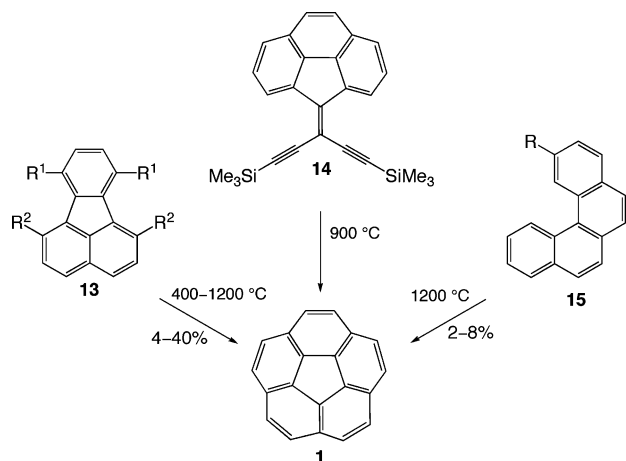
produces 5,5-dicarbethoxy-6-carboxy-3-oxo-3,4,5,5a-tetrahydrobenzo[ghi]fluoranthene **8**, which upon hydrogenation over palladium on charcoal gives dodecahydro diester acid **9** in excellent yield. Esterification of **9** with diazomethane

Chart 1

Scheme 1. Synthesis of Corannulene **1** Based on Lawton and Barth's Procedure⁶

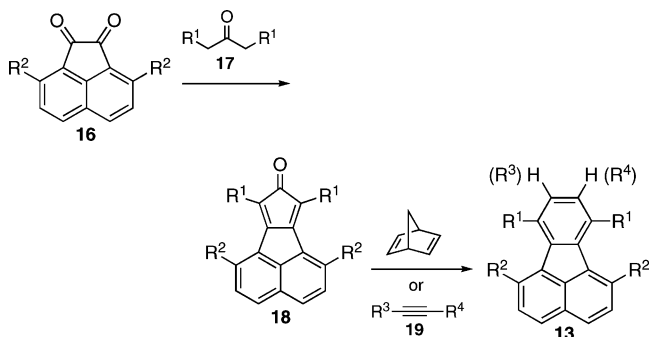
followed by Acyloin condensation produces the acyloin ester **10**. Sodium borohydride reduction of **10** followed by hydrolysis with potassium hydroxide in *n*-propyl alcohol produces the diol acid **11**, which can be converted to **12** upon acid dehydration followed by thermal decarboxylation. Sodium borohydride reduction of the ketone and subsequent aromatization over palladium on charcoal leads to corannulene **1** (17 linear steps, <1% overall yield). This classic work was a tour de force in PAH synthesis and started the field of Eulerean carbon surfaces; however, the lengthy synthesis and overall low yield limited further study of corannulene.

A few years latter, high-temperature pyrolysis routes provided another possibility to achieve novel strained PAH target molecules (Scheme 2 and Table 1). One key reaction for the history and development of corannulene derivatives was the synthesis of acenaphthalene from ethynynaphthalene by Roger Brown.⁹ This reaction suggested the possibility of using the rearrangement of the ethynyl unit to a vinylidene reactive intermediate. Ingeniously, Larry Scott saw how to use this rearrangement to prepare **1** in an incredibly short synthesis from commercially available starting materials; his success sparked many others to join in the field.¹⁰

Scheme 2. Access to Corannulene (1) by Pyrolysis from Different Starting Materials

Table 1. Preparation of Corannulene by Pyrolysis Routes

entry	S.M.	substituents	temp. [°C]	yield (%)	ref
1	13a	R ¹ : -C≡CH, R ² : H	1000	10	10a
2	13b	R ¹ : -C≡CSiMe ₃ , R ² : H	1000	36	10b
3	13c	R ¹ : C(OSiMe ₃)=CH ₂ , R ² : H	1000	8	10c
4	13d	R ¹ : CH=CHCl, R ² : H	1100	35–40	10d,e
5	13e	R ¹ : CH=CBR ₂	700–1000	4–23	10e,f
6	13f	R ¹ = R ² = CH ₂ Br	1000	18	10g
7	13g		400	7	10g
8	15a	R: -C≡CH	1200	2–4	12
9	15b	R: CCl=CH ₂	1200	8	12
10	15c	R: CH=CHCl	1200	8	12
11	15d	R: C(OSiMe ₃)=CH ₂	1200	2–4	12

This practical and efficient method developed by Scott et al. required three steps and produces **1** in a total yield of 26%.^{10e} In the first step, the three starting materials, i.e., **16** (R² = H), 2,4,6-heptanetrione (**17**, R¹ = Ac), and norbornadiene, are heated with the catalyst, glycine, in toluene (Scheme 3). The Knoevenagel condensation between **16** and

Scheme 3. Synthesis of Fluoroanthrene Derivatives **13 by Knoevenagel Condensation and Sequential Diels–Alder Reaction from Acenaphthenequinone **16**, Ketone **17**, and Norbornadiene (or Alkyne **19**)**


17 affords the cyclopentadienone derivative **18** (R¹ = Ac, R² = H), which undergoes Diels–Alder reaction with norbornadiene (or alkyne **19**) *in situ* to give 7,10-diacetylfluoroanthrene **13** (R¹ = Ac, R² = H) after loss of a carbon monoxide and cyclopentadiene. Transformation of the two methyl ketones in the side chains of **13** to chlorovinyl groups occurs in 85% yield by treatment of **13** with PCl₅. Pyrolysis of **13d** (Table 1; Entry 4) at high temperature yields corannulene (**1**), presumably via a diethynyl intermediate

produced by loss of hydrogen chlorides. Scott envisioned that terminal acetylenes would rearrange to vinylidene carbenes under these conditions and that the carbenes would insert into the CH bonds of the naphthalene fragment to close the two six-membered rings.^{10e,f}

Other groups have devised pyrolysis precursors like fluoroanthrenes **13**,¹⁰ cyclopenta[*def*]phenanthrenes **14**,¹¹ and benzo(*c*)phenanthrenes **15**¹² to prepare **1**. In most cases, these pyrolysis routes do not provide **1** in high yields or appreciably large scales. Nonetheless, Scott has been a master at crafting pyrolysis routes to curved aromatic surfaces (cf. section x of this issue).

Although the obvious success of the preparation of corannulene by the FVP strategy comes from the small number of steps, the strategy suffers from several drawbacks: (1) modest yields, (2) almost no functional group tolerance, (3) small scale runs, and (4) potential for thermal rearrangements of the molecule framework at high temperatures (1000–1300 °C) to lead to undesired products.¹³ Thus, synthesis of corannulene (**1**) under mild synthetic conditions (in solution phase) became an important goal.

In an early attempt to this goal, Siegel and co-workers developed a method that started from 3,8-dimethylacenaphthene-1,2-dione (**16**, R² = Me), 3-pentanone, and norbornadiene to afford 1,6,7,10-tetramethylfluoroanthrene **20** via, again, Knoevenagel condensation and sequential Diels–Alder reaction.^{10g} Selective bromination of **20** to the tetrabromide was possible, but Wurtz-type couplings were not observed. At that point pyrolysis was used to finish the synthesis.

The first published example of a corannulene derivative made by a wholly solution-phase synthesis was reported by Siegel and co-workers a few years later.¹⁴ Therein 2,5-dimethylcorannulene was prepared en route to a corannulene cyclophane. The synthesis used the same path introduced by Siegel and co-workers in 1992 to get to a 1,6,7,10-tetraalkylfluoroanthrene,^{10g} but by substituting 4-heptanone for 3-pentanone they were able to show that additional substituents could be introduced. Two key points followed: (1) benzylic bromination gave the tetrabromide and (2) a reductive coupling strategy to close the carbon–carbon bond across the 1,10 and 6,7 positions followed by dehydrogenation was introduced in place of a pyrolysis. Thus, this synthesis showed that solution-phase methods could introduce substituents regioselectively, which was not possible by pyrolysis methods.

Siegel's methodology for producing 2,5-dimethylcorannulene was applied later independently by Rabideau¹⁵ and Siegel¹⁶ (Scheme 4 and Table 2) for the synthesis of the corannulene parent compound. Both research groups brominated **20** with NBS under forcing condition to produce octabromide **21**, which undergoes ring closure with the reducing agents in an anhydrous condition (Method A, Scheme 4).

In a further refinement to the synthesis, Sygula and Rabideau discovered an appealing alternative method to 1,2,5,6-tetrabromocorannulene **23** from **21** by use of sodium hydroxide to deprotonate the remaining benzylic hydrogen and initiate carbon–carbon bond formation.¹⁷ The reaction is solvent dependent but can be done on a large scale. The desired molecule **1** (≡ **22a**, R = H) is formed by treatment of **23** (R = H) with zinc and potassium iodide (Method B, Scheme 4).

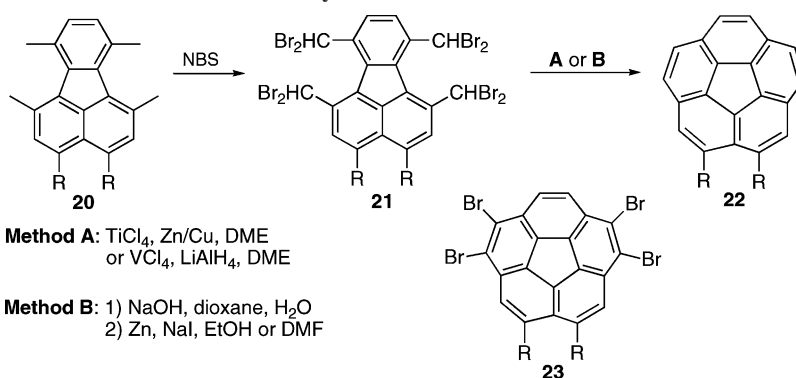
Scheme 4. Preparation of Corannulene Derivatives **22** by Solution Methods

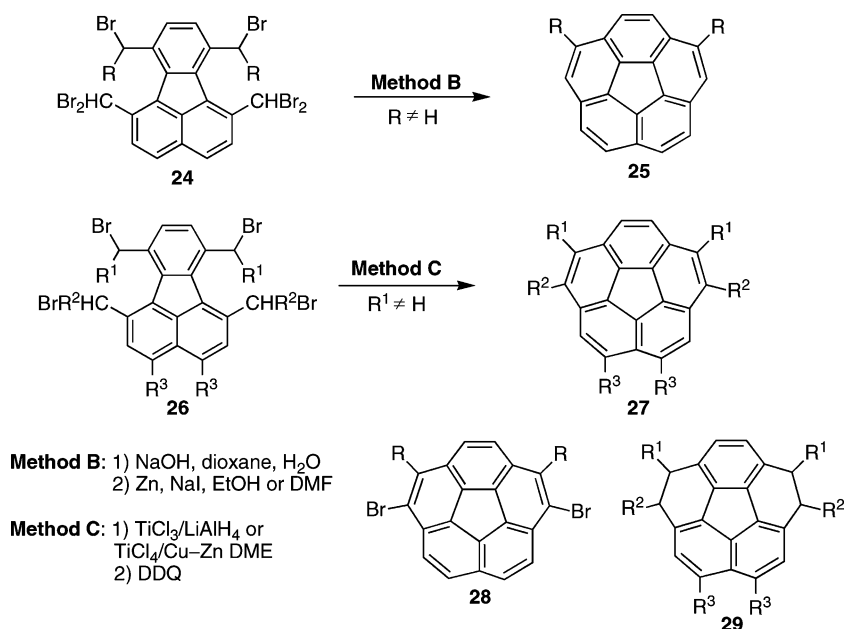
Table 2. Synthesis of Various Corannulene Derivatives in Solution Phases

entry	product	substituents ^a	method	yield (%)	ref
1	22a (\equiv 1)	R = H	A ^a	80	16
2	22a (\equiv 1)	R = H	A ^b	70–75	15
3	22a (\equiv 1)	R = H	B	74	17
5	22b	R = Cl	A	85	16
6	25a	R = Me	B	66	18
7	28a	R = 2-Br-Ph	B	96	19
8	27a	R ¹ = Me, R ² = H, R ³ = H	C	24	16
9	27b	R ¹ = H, R ² = Me, R ³ = H	C	48	16
10	27c	R ¹ = H, R ² = Me, R ³ = Cl	C	45	16
11	27d	R ¹ = R ² = Me, R ³ = H	C	6	16
12	31a	R ¹ = R ² = CO ₂ Me	D	60	22
13	31b	R ¹ = R ² = CO ₂ Me, R ³ = Cl	D	49	20
14	31c	R ¹ = Ph, R ² = CO ₂ Me, R ³ = Cl	D	51	20

^a TiCl_4 , Cu–Zn procedure. ^b VCl_3 , LiAlH_4 procedure.

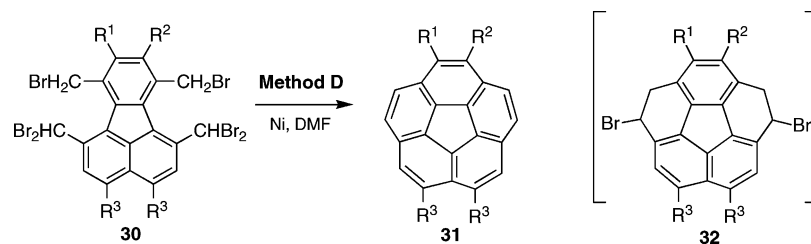
Under forcing bromination conditions, octabromides (i.e., **21**) form from 1,6,7,10-tetraalkylfluoranthenes **20** bearing no flanking ortho substituents. Hexa- and tetrabromides **24** and **26**, respectively, are obtained as a function of the steric hindrance of the flanking functional groups. Extension of the 1,6,7,10 alkyl substituents (for example, to ethyl) also limits the degree of bromination. Nonetheless, ring closure of tetra- and hexabromides to corannulene derivatives can be achieved by a variety of different procedures and lead regioselectively to substituted corannulene derivatives.

Scheme 5. Formation of Corannulene Derivatives from Hexa- and Tetrabromofluoroanthene Derivatives



Method B is analogous to Sygula and Rabideau's base-promoted ring closure and converts hexabromides **24** to brominated derivatives of type **28**, which upon reduction give corannulene derivatives **25** (Scheme 5 and Table 2). Method C was originally introduced by Siegel's group on the basis of reductive benzylic coupling chemistry pioneered by Prakash and Olah.²¹ This procedure first generates tetrahydrocorannulene derivatives **29** from tetrabromides **26** under reductive conditions. Subsequent oxidation of **29** affords the desired corannulene derivatives **27**.¹⁶

Although methods A–C are efficient to generate corannulene derivatives, they would be problematic for sensitive functionality like the ester moiety. For example, cyclization of precursors **30** ($\text{R}^1 = \text{R}^2 = \text{CO}_2\text{Me}$) is doomed to failure under the reduction conditions of method A and C or in the presence of aqueous base as in method B. A new protocol developed by Sygula et al. forms the corannulene core by a nickel-mediated intramolecular coupling of benzyl and benzyldene bromides (Method D, Scheme 6).²² In contrast to above other methods, this protocol provides higher tolerance of functional groups, especially esters. Closure of two six-membered rings leads to completely debrominated products **31**. According to the postulated mechanism for nickel-mediated reductive coupling of benzyl/benzyldene bromide,^{23,24} the dibromide **32** should be formed; however, **32** is not observed, probably due to a spontaneous double elimination of HBr leading to **31**.

Scheme 6. Preparation of Corannulene Derivatives **31** by Ni-Mediated Cyclizations

Scheme 7. Synthesis of Monosubstituted Corannulenes

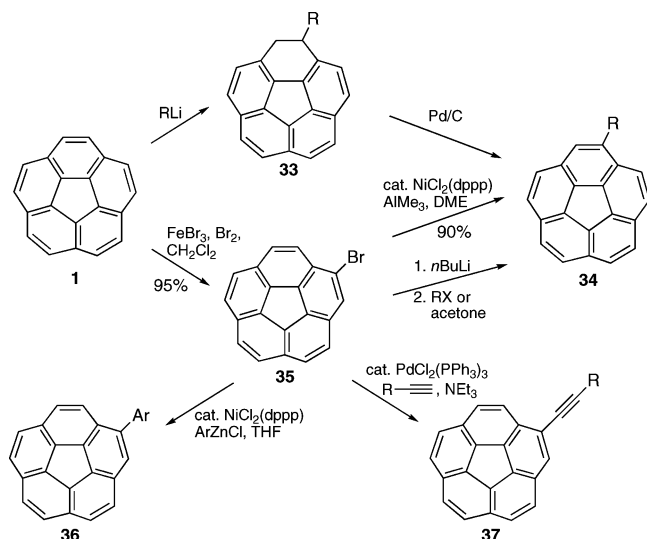


Table 3. Photophysical Properties of Some Monosubstituted Corannulenes

entry	R	product	yield (%)	λ_a , nm ^c	λ_f , nm ^c	Φ_f ^c
1	SiMe ₃	37a	97	376 ^{sh} , 334 ^{sh}	426, 407 ^{sh}	0.14
2	Ph	37b	67	400, 356	429, 409	0.31
3	H	37c	quant. ^a	389, 381 ^{sh}	426, 409 ^{sh}	0.08
4	corannulenyl	37d	45	410, 386 ^{sh}	440, 418	0.57
5	F ₃ Ph	37e	57 ^b	398, 356	431, 411 ^{sh}	0.26

^a Yield is calculated for the desilylation of **37a**. ^b Reaction of **37c** and iodoperfluorobenzene. ^c Measurements in cyclohexane.

Monoalkyl-substituted corannulene **34** can be accessed from corannulene **1** by alkylation and subsequent dehydrogenation. Intermediates, 1-alkyl-1,2-dihydrocorannulenes **33a** (R = *i*Pr) and **33b** (R = *t*Bu), are generated upon treatment of **1** with the corresponding organolithium reagents in good to excellent yields (Scheme 7).²⁵ X-ray diffraction analyses of both compounds in the solid state exhibit bulky substituents in the *exo*-pseudoaxial location. However, methyl-lithium does not give **33c** (R = Me) under the same conditions.

Bromocorannulene **35** is prepared from corannulene and bromine in the presence of a Lewis acid catalyst.²⁶ Methylcorannulene **34c** (R = Me) can be prepared from **35** by treatment with trimethylaluminum in the presence of NiCl₂(dppp) as catalyst.¹⁶ Monoaryl- and monoalkynyl-substituted corannulenes **36** and **37** are also accessible from **35** by Negishi couplings²⁷ and Sonogashira reactions,²⁸ respectively (Table 3). Conversion of **35** with *n*BuLi to the corannulyl lithium species and quenching with alkylation agents (RX or acetone) also affords the corresponding **34** derivative.^{10f}

The bucky bowl aryne **38** has been prepared by Sygula et al.²⁹ Treatment of **35** with an excess of NaNH₂ and a catalytic

amount of *t*BuOK in THF at room temperature forms corannulyne **38**, which can be trapped by diphenylisobenzofuran or furan to generate Diels–Alder products **39** and **40**, respectively, in good yields (Scheme 8). *N,N*-Diisopropylaminocorannulene **42** is also accessible by nucleophilic addition of *N,N*-diisopropylamine to *in-situ*-generated **38**. Refluxing with Fe₂(CO)₉ in benzene converts **40** quantitatively into benzocorannulene **41** by cleavage of the ‘end-oxide’ bridge.

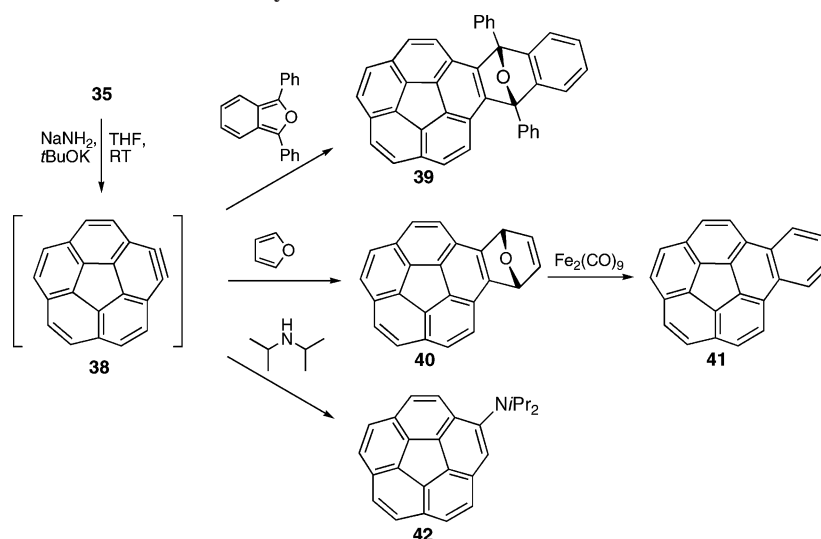
Dichlorocarbene reacts with corannulene first at the fused 6:6 bond to form **43** but can react further to give a diadduct **44** (Scheme 9).³⁰ No addition is seen at the rim alone **45** nor at the 6:5 ring fusion. Selective attack at the 6:6 ring fusion is reminiscent of the reaction of dichlorocarbene with C₆₀. Reaction of phenanthrene and dichlorocarbene produces **46**. Formation of cyclopropane **43** is suggested as a stepwise mechanism. No direct experimental evidence supports this hypothesis, but indirect support comes from the fact that thermal decomposition of **43** in the presence of cyclohexene leads to corannulene and 3,3'-dicyclohexenyl. If the C–C bond in the cyclopropane moiety of **43** breaks to generate diradical **47**, which abstracts hydrogen from cyclohexene to produce radical **48**, then formation of corannulene could ensue by loss of HCCl₂ radical; 3,3'-dicyclohexenyl would form concomitantly by dimerization of the cyclohexenyl radical.

Siegel and co-workers prepared 2,3-disubstituted corannulene derivatives **49–52** by an alternative synthesis, which starts from acenaphthalene and proceeds via 1,6-dibromo-3,4-dichloro-7,10-dimethylfluoranthene to **22b** (Scheme 10).³¹ Treatment of **22b** with trimethylaluminum in the presence of NiCl₂(dppp) yields 2,3-dimethylcorannulene (**49**), from which the bis(bromomethyl) derivative **50** can be produced by benzylic bromination with *N*-bromosuccinimide. Similar treatment of **22b** with phenylmagnesium bromide in the presence of NiCl₂(dppp) yields 2,3-diphenylcorannulene (**51**). Heating **22b** in diethylene glycol monomethyl ether with an excess of sodium hydride effects a nucleophilic aromatic substitution to form the 2,3-bis(diethylene glycol methyl ether) derivative **52**.

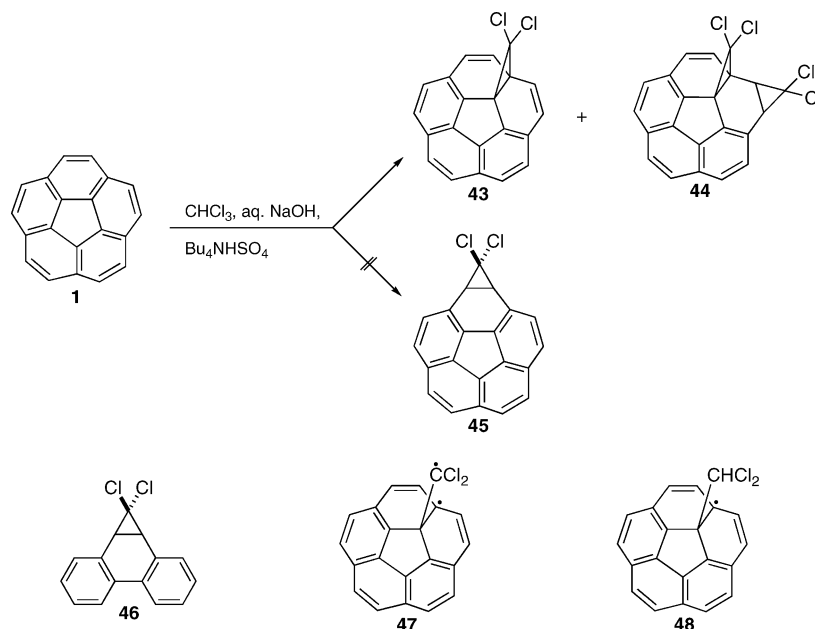
2.1.2. Structure and Properties

The C–C bonds in corannulene are conveniently classified as Rim, Flank, Hub, and Spoke (Scheme 11).^{10g} X-ray crystallographic analysis of **1** shows a bowl depth of 0.87 Å,³² as measured from the plane containing the five-membered ring to the plane containing the peripheral aromatic carbon atoms, and this is significantly more shallow than would be expected for the polar cap within C₆₀ (ca. 1.5 Å).³³ Curvature of corannulene is analyzed by the POAV (π -orbital axis vector) pyramidalization angle.³⁴ The POAV pyramidalization angle of the carbon on the central five-membered ring (hub) is 8.2°, in contrast to 11.6° for C₆₀. The rim carbons are predicted to be only slightly pyramidalized with pyramidalization angles in the range of 1–2°.

Scheme 8. Generation and Reactions of Corannulyne 38



Scheme 9. Reaction of Dichlorocarbene with Corannulene



Unlike the crystal structures of pyrene and related aromatic compounds of comparable surface area, the crystal structure of **1** is void of any aromatic face-to-face or bowl stacking.

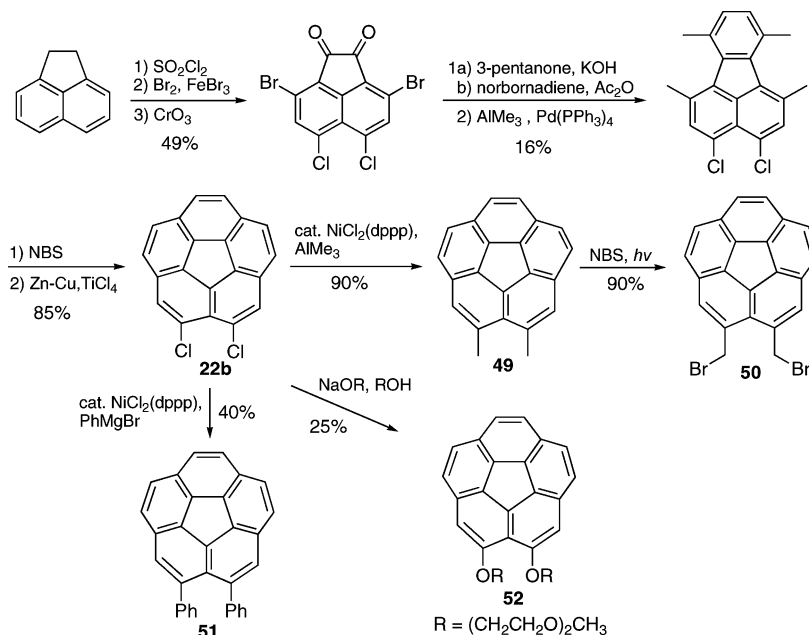
Corannulene (**1**) is known for its bowl shape. Its bowl-to-bowl inversion process is defined as bowl form **1** converting to form **1'** via a transition structure **1[‡]** (Figure 1). The difference in energy between **1** and **1[‡]** represents the bowl inversion energy ($\Delta G_{\text{inv}}^\ddagger$), which can be measured experimentally by variable-temperature ^1H NMR study of suitably substituted corannulenes **34**. Values for $\Delta G_{\text{inv}}^\ddagger$ depend on the substituent R with benzyl-,³⁵ isopropyl-,³⁵ and bromomethylcorannulene³¹ exhibiting a higher $\Delta G_{\text{inv}}^\ddagger$ than 1-corannulenyl-1-methyl-1-ethanol (Table 4).^{10f} The experimental value of $\Delta G_{\text{inv}}^\ddagger$ for the nonsubstituted parent **1** is estimated as 11.5 kcal/mol, although in achiral media it cannot be directly measured due to symmetry.³⁶

As the hydrogens of the *peri* positions in **1** are replaced by larger moieties the repulsion energy should increase and $\Delta G_{\text{inv}}^\ddagger$ should decrease relative to that for **1**. Determination of the $\Delta G_{\text{inv}}^\ddagger$ of some 2,3-disubstituted corannulenes tested

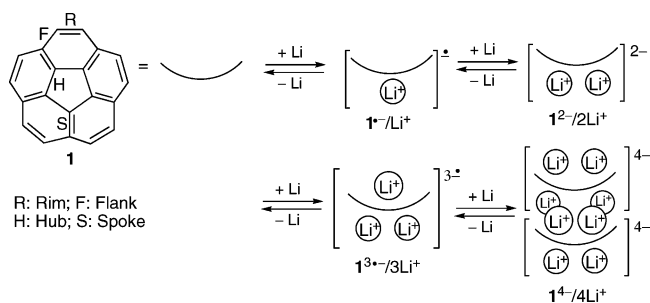
this hypothesis (Table 5).^{31,36} The order of barrier heights follows oxygen (**52**) > phenyl (**51**) > bromomethyl (**50**) > chlorine (**22b** calcd; **55** exptl), but all the preceding exhibit lower barriers than other disubstituted corannulene derivatives, like **53** and **54** (Chart 2), for which there is no special *peri* X/X repulsion. Clearly, *peri* repulsions flatten the bowl and cause a decrease in $\Delta G_{\text{inv}}^\ddagger$.

Reduction of corannulene (**1**) at -78°C with excess lithium metal in THF- d_8 over a period of several days leads to a series of three color changes, first to green, then to purple, and finally to brownish-red.³⁷ Quenching this solution with water affords tetrahydrocorannulene as the major product accompanied by lesser amounts of dihydrocorannulene and corannulene. The reduction states of corannulene (Scheme 11) lie between the neutral hydrocarbon and the tetraanion ($\text{1}^{4-}/4\text{Li}^+$) via the radical monoanion ($\text{1}^{\bullet-}/\text{Li}^+$), dianion ($\text{1}^{2-}/2\text{Li}^+$), and trianion ($\text{1}^{3-}/3\text{Li}^+$). These intermediates and final product were characterized by NMR and EPR.³⁷ A pronounced counterion effect on the chemical reduction is observed. Reduction to the corannulene trianion

Scheme 10. Synthesis of 2,3-Disubstituted Corannulenes



Scheme 11. Schematic Presentation of Li–Corannulene Complexes



and tetraanion can be achieved with lithium, whereas reduction with the larger potassium stops at the dianion stage. The corannulene tetraanion exists as a stable diamagnetic species due to the unexpected aggregation to form a high-order molecular sandwich with four lithium atoms between the two corannulene tetraanions.³⁸

Recently, Morita et al. reported the first bowl-shaped neutral radical **58**, which is prepared from corannulene **1** in four steps via aldehyde **56** and tetrahydrotetrazine derivative **57** (Scheme 12).³⁹ Radical **58** was obtained as a vivid red

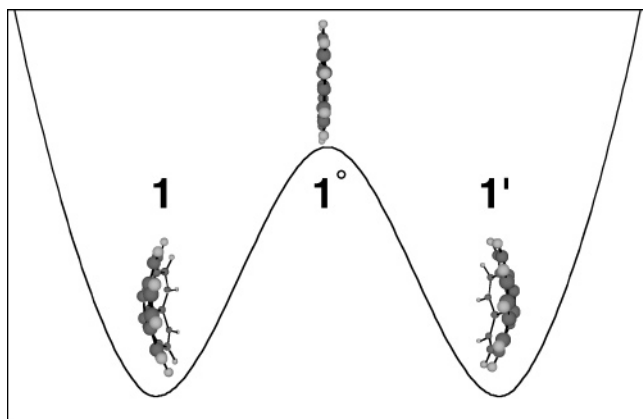


Figure 1. Energy diagram of the bowl-to-bowl inversion process of **1**. Reprinted with permission from ref 31. Copyright 2001 American Chemical Society.

Table 4. $\Delta G_{\text{inv}}^{\ddagger}$ for monosubstituted Corannulenes **34**

compd.	R	coalescence temp. (K)	$\Delta G_{\text{inv}}^{\ddagger}$ (kcal/mol)	ref
1			11.5 ^a	31, 36
1			9.2 ^b	31, 36
34a	C(CH ₃) ₂ OH	209	10.2	10f
34b	C(CH ₃) ₂ H	242	11.3	35
34c	CH ₂ Br	223	11.0	31
34d	CH ₂ Ph	234	11.2	35

^a Experimental estimate. ^b B3LYP/cc-pVDZ.

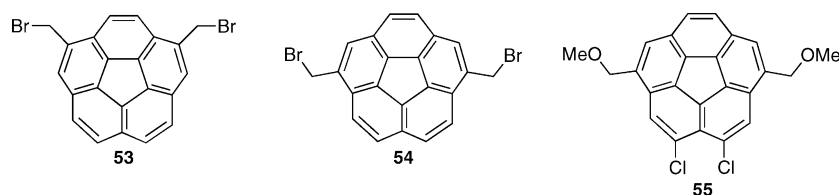
Table 5. Inversion Barrier ($\Delta G_{\text{inv}}^{\ddagger}$) and Bowl Depth of *peri*-Substituted Corannulenes^{31,36}

compd.	MP2/cc-pVDZ (sp)		RHF/cc-pV DZ		B3LYP /cc-pV DZ	
	exp. $\Delta G_{\text{inv}}^{\ddagger a}$	$\Delta G_{\text{inv}}^{\ddagger a}$	$\Delta G_{\text{inv}}^{\ddagger a}$	bowl depth ^b	$\Delta G_{\text{inv}}^{\ddagger a}$	bowl depth ^b
51	9.4					
52	9.9					
53	10.4					
27a		11.1	9.1	0.825	9.0	0.866
54	10.5					
27b		11.1	9.1	0.825	9.0	0.865
55	8.7					
22b		9.1	7.5	0.782	7.4	0.822
50	9.1					
49		9.6	7.7	0.789	7.7	0.830

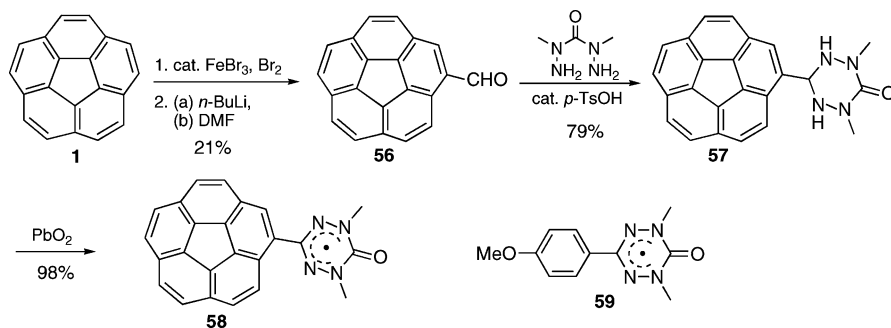
^a Units: kcal/mol. ^b Units: Å.

powder, stable in the solid state in air and degassed toluene for long periods. The *g* values of **58** and **59** are the same (*g* = 2.0041). Experiment and computation (DFT method) indicate that most of spin density is localized on the oxoverdazyl moiety. Compared to the corannulene absorption bands in the region 220–300 nm, the peak maxima of **58** shift only 3–6 nm, indicating that the π conjugation between the corannulene moiety and the oxoverdazyl unit is weak. The reduction potentials of **1** and **58** by cyclic voltammetry are nearly identical. Radical **58** displays an irreversible oxidation wave at + 0.24 V (vs Fc/Fc⁺), whereas radical **59** shows a reversible signal at the same potential.

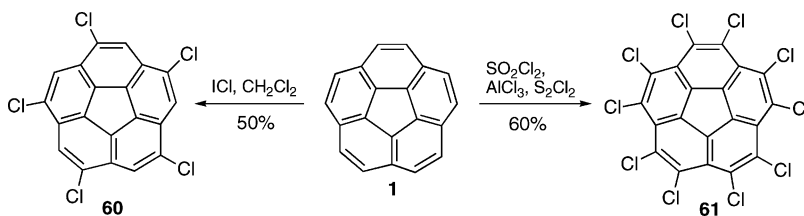
Chart 2



Scheme 12. Stable Neutral Radical 58



Scheme 13. Synthesis of Penta- and Decachlorocorannulene



2.2. Highly Substituted Corannulenes

2.2.1. Synthesis

Direct multiple electrophilic aromatic substitution on corannulene has shown limited but important successes. Friedel–Crafts alkylation is able to introduce five sterically bulky groups like *tert*-butyl in a symmetrical fashion, but general alkylation, acylation, or halogenation leads to products with various degrees of substitution and as mixtures of isomers.²⁶ Two special chlorination procedures enable study this area (Scheme 13). (1) Balister conditions, using sulfonyl chloride, aluminum chloride, and sulfur dichloride, produce a sparingly soluble decachlorocorannulene **61**,⁴⁰ albeit a very difficult product to purify. (2) A curious reaction between ICl and **1** leads to roughly 50% of the *sym*-1,3,5,7,9-pentachlorocorannulene **60**.⁴¹ Already mentioned above, 1,2,5,6-tetrabromocorannulene **23** (R = H) is a formal precursor of corannulene when using the Sygula/Rabideau closure. In the context of discussing the synthesis of corannulyl halides, it is worth mentioning that tetrabromide **23** can undergo halogen-exchange reactions to form the corresponding iodide **62** (Scheme 14), also a precursor of **1**.¹⁷ Arguably **23** and **62** are however even more important to making corannulene derivatives than it is to making the parent **1** (\equiv **22a**, R = H, Scheme 4).

The importance of halogen derivatives **23**, **22b**, **60**, **61**, and **62** stems from the variety and reliability of nucleophilic aromatic substitutions and related transition-metal-mediated couplings of nucleophiles with aryl halides. Already introduced in the chemistry of the 2,3-dichlorocorannulenes like **22b**,¹⁶ this chemistry transfers well with minor modifications to other halogenated corannulenes. Preparations of tetraethynylcorannulene derivatives **63** are accessible by Sono-

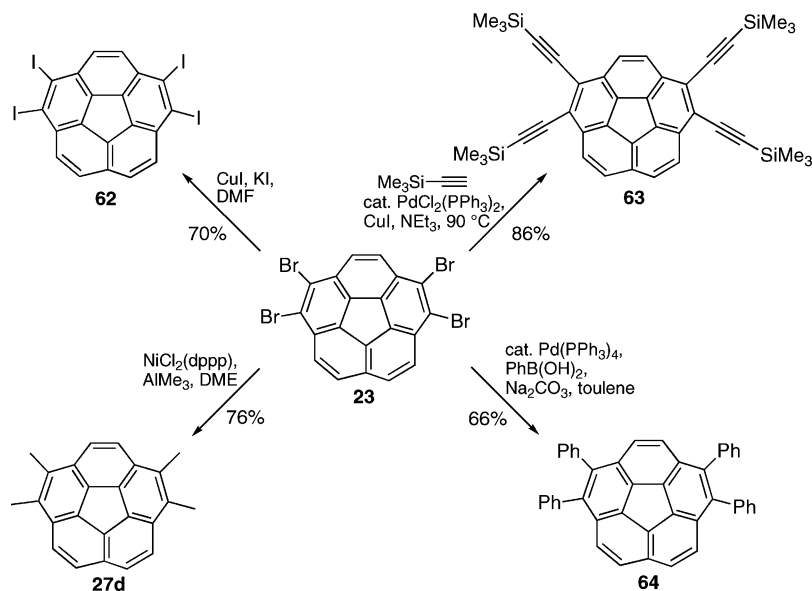
gashira reactions.¹⁷ Additionally, tetramethyl- and tetraphenylcorannulene **27d** and **64**, respectively, can be also obtained from **23** by Ni-catalyzed methylation and Suzuki coupling in good yields.^{17b–c}

It is well known that the cross-coupling reactions of aryl chlorides with various reagents are much more difficult than the corresponding bromide. Thus, 1,3,5,7,9-pentasubstituted corannulenes from **60** presented several major challenges, among them overcoming the sparing solubility, activating the chloride for substitution, and completing the reaction five times on each molecule. Developing effective synthetic methods for coupling reactions with **60** is an accomplishment on par with the most difficult substrates. Despite the expected low yields and poor reactivity, several solutions to this problem have been found.

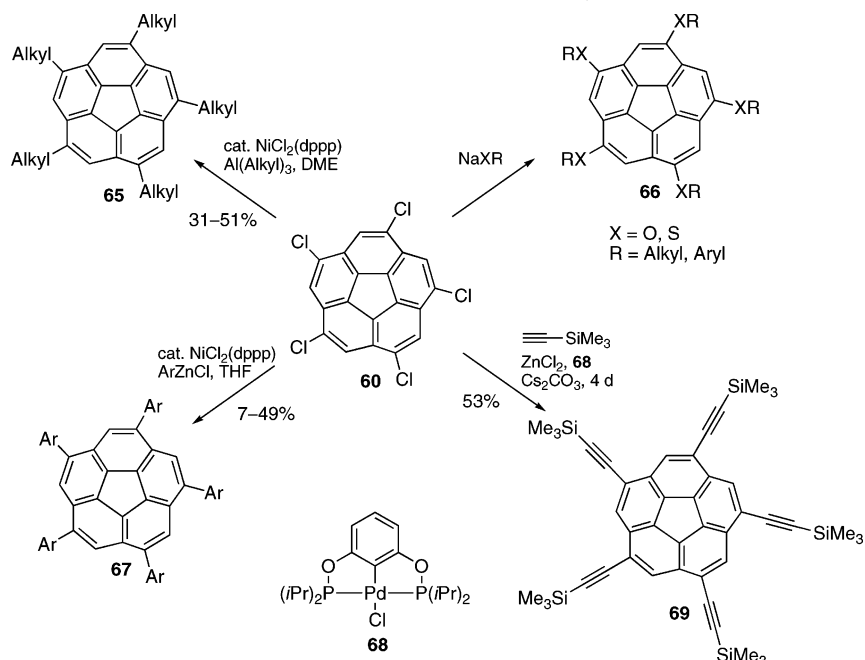
Pentaalkylcorannulenes **65** and pentaarylcorannulenes **67** are accessible by alkylation and arylation of **60** in the presence of NiCl₂(dppp) catalyst with organoaluminium and organozinc reagents, respectively (Scheme 15, Table 6).⁴² The extremely low yield of coupling product **67c** likely stems from the steric hindrance of the two ortho methyl groups in the manisyl moiety. Implementation of more stable palladium catalysts based on N-heterocyclic carbenes, ala Nolan,⁴³ allow higher reaction temperatures and result in better yields in these sterically congested cases.

Direct nucleophilic substitution of **60** is possible to produce **66** in the presence of nucleophiles without any catalysts, even at 25 °C. Treatment of **60** with sodium arylthiolates in DMEU (= dimethylethanourea) at ambient temperature (for **66a** and **66b**)⁴⁴ or at 120 °C (for **66c**)⁴² gives 1,3,5,7,9-pentakis(arylthio)corannulene derivatives. Pentakis(1-thia-propyl)corannulene **66d** is also accessible by the same method. Formation of **66e** from reaction of **60** and the

Scheme 14. Synthesis of 1,2,5,6-Tetrasubstituted Corannulenes



Scheme 15. Synthesis of Pentasubstituted Corannulene Derivatives (for details, see Table 6)



corresponding sodium alkoxide requires high temperature (180 °C).⁴² The mechanism of these direct nucleophilic substitution for generation of **66** should be via a Meisenheimer complex⁴⁵ rather than an aryne intermediate.

1,3,5,7,9-Pentakis(trimethylsilylethynyl)corannulene (**69**)⁴² is prepared from pentachloride **60** and a large excess (ca. 50 equiv) of trimethylsilylethyne using Eberhard's method⁴⁶ with the pincer catalyst **68** at high temperature (ca. 165 °C).

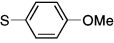
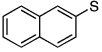
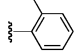
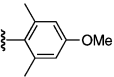
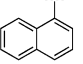
Decamethylcorannulene **70** is obtained in 30% yield by methylation of **61** in the presence of NiCl₂(dppp) and trimethylaluminum (Scheme 16).³⁶ The possibility to replace chlorine with sulfur by a nucleophilic aromatic reaction is general for **61** and a variety of S-nucleophiles. Indeed, Scott et al. prepared various decakis(1-alkylthio)corannulenes **71a–c** and pentakis(1,4-benzodithiino)corannulene (**71d**) from decachlorocorannulene (**61**) and the corresponding sodium thiolates at room temperature in good yields.⁴⁷

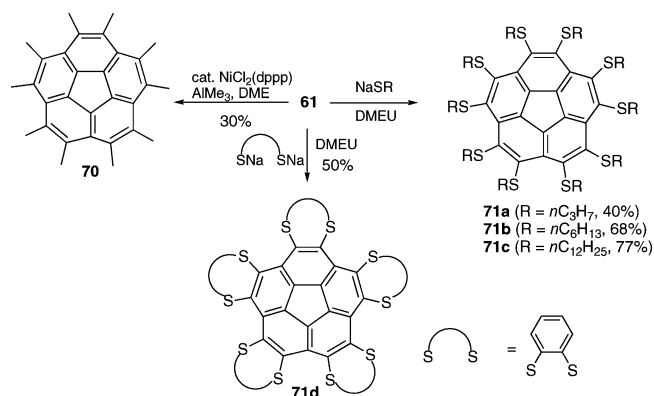
2.2.2. Structures and Properties

The calculated value of $\Delta G_{\text{inv}}^{\ddagger}$ for **65a** is 8.7 kcal/mol, and its bowl depth is 0.85 Å (Table 7).^{31,36} The calculated value of $\Delta G_{\text{inv}}^{\ddagger}$ for **70** is 2.2 kcal/mol, and its bowl depth is 0.58 Å.^{31,36} Both compounds conform well to the bowl-depth/inversion barrier relationship described above. $\Delta G_{\text{inv}}^{\ddagger}$ for **67c** is experimentally determined to be ca. 12.1 kcal/mol, which is about 2.5 kcal/mol higher than expected based on its bowl depth and 0.5 kcal/mol higher than the calculated barrier for the parent **1**. The increase of the barrier height has been assumed to come from van der Waals attractive forces among the endo methyl groups in the conformational ground state of **67c**; these interactions are not present in the bowl-inversion transition state, and overcoming them adds to the overall inversion barrier.⁴⁸

The attached methyl groups in **65a** and **70** not only flatten the corannulene cores, but also increase electron density in

Table 6. Selected Examples of Pentasubstituted Corannulene Derivatives

Entry	Alkyl/XR/Ar	Product	Yield (%)	λ_c , nm	λ_r , nm
1	Me	65a	33	295	431
2	Et	65b	51	297	431
3		66a	50		
4		66b	55		
5	SPh	66c	38	349	
6	SEt	66d	37	337	
7	O(C ₂ H ₅) ₂ Me	66e	41	308	433
8	Ph	67a	49	319	447
9		67b	28	308	440
10		67c	7	305	439
11		67d	38	311	445
12	SiMe ₃	69	53	337, 366 ^h	474

Scheme 16. Preparation of Decasubstituted Corannulenes

the corannulene nucleus. It is consistent with the electrochemical measurement that the reduction potential for the monoanion of **65a** and **70** is more negative than that of **1** by 150 and 250 mV, respectively.¹⁶ Additionally, the computational results at the RHF/DZV(2d,p)/B3LYP/cc-pVDZ level using Koopman's theorem predict ionization potentials for **65a** (7.71 eV) and **70** (7.19 eV) that are smaller than that for **1** (8.05 eV). Like electrochemical reduction, the shift to lower ionization potential arises from an increase of electron density in the corannulene nucleus by the methyl groups at the *rim* of corannulene.

An X-ray crystal structure of **71d** reveals that two molecules of the 'fly trap' surround one molecule of benzene in this crystal (Figure 2, left).⁴⁷ This result indicates the possibility for formation of supramolecular complexes with the fullerene family. The convex surface of C₆₀ is electron deficient (good π -acceptor), whereas compound **71d** is electron rich. A π -donor/ π -acceptor complex forms by treatment of **71d** with C₆₀ and C₇₀ (ratio 1:1) in carbon disulfide. The K_{assoc} values (ca. 1420 and 1080 M⁻¹, respectively) were determined using ¹H NMR techniques.⁴⁹

Table 7. Inversion Barrier and Bowl Depth of Some Highly Substituted Corannulenes

compd.	MP2/cc-pVDZ (sp)		RHF/cc-pVDZ		B3LYP/cc-pVDZ		
	exp. $\Delta G_{\text{inv}}^{\ddagger a}$	bowl depth ^b	$\Delta G_{\text{inv}}^{\ddagger a}$	$\Delta G_{\text{inv}}^{\ddagger a}$	bowl depth ^b	$\Delta G_{\text{inv}}^{\ddagger a}$	bowl depth ^b
65a			11.3	8.9	0.81	8.7	0.85
67c	12.1	0.94					
70			1.3	2.0	0.54	2.2	0.58

^a Units: kcal/mol. ^b Units: Å.

The calculated structure of complex **71**:C₆₀ is shown in Figure 2. However, K_{assoc} values of the complexations with C₆₀ for the less congested derivatives **66a** and **66b** are obviously smaller than **71d**.⁴⁷

The crystal form of the decathio compound displays an alternating up/down out-of-plane conformation for the phenylthio substituents. As known for other perthioaromatics, the perthiophenylcorannulene **66c** is much easier to reduce than the parent, displaying a reduction potential close to that for C₆₀.

2.3. Cyclopentacorannulene, Acecorannulene, and *peri*-Annulated Corannulenes

2.3.1. Synthesis

Cyclopentacorannulene (**73**) was first prepared as a mixture with corannulene (in ratio 7:3) in 10–15% yield from dichloride **72** by flash vacuum pyrolysis at 1000 °C (Scheme 17).⁵⁰ Later, Siegel and co-workers synthesized **73** from **74** in the solution phase in 20% yield by titanium-mediated carbenoid couplings.¹⁶

Acecorannulene (**75**) can be generated from cyclopentacorannulene (**73**) by hydrogenation in excellent yield (Scheme 18).⁵⁰ Alternatively, **75** is produced from dibromide **50** in ca. 20% yield by either palladium-catalyzed Stille-type coupling³⁶ or treatment with phenyllithium.³¹

Various (heterocyclic) six-membered *peri*-annulated corannulene **76–80** derivatives are accessible from reaction of divalent nucleophiles with 2,3-bis(bromomethyl)corannulene (**50**) (Scheme 19).³¹ The sulfide **76** can be synthesized by treatment of **50** with sodium sulfide nonahydrate. The malonate derivative **77a** is prepared by condensation of **50** with diethylmalonate in an ethanolic solution of sodium ethoxide. Reaction of amines with sodium hydride and **50** produce the aza derivatives **78**. The selenide **79** is generated in one pot by reaction of 1 equiv of potassium selenocyanate with **50** followed by *in situ* generation of the selenide anion with sodium borohydride and ring closure. Treatment of **50** with potassium hydroxide in 1,2-dimethoxyethane affords the ether derivative **80**.

2.3.2. Structures and Properties

The crystal structure of **73** is determined to have a bowl depth of ca. 1.054 Å.⁵¹ The POAV pyramidalization angles for the carbon atoms in **73** calculated from the crystal structure and *ab initio* HF/6-31G* geometries are larger than those for **1** (Figure 3). Annulation of a five-membered ring to the rim of the corannulene carbon framework increases significantly the curvature and rigidity of the system.

Computational studies of $\Delta G_{\text{inv}}^{\ddagger}$ for **73** and **75** predict values of 27.7–30.9 and 25.6–28.9 kcal/mol, respectively (Table 8).⁵² These results are consistent with the fact that **75** is less bowl-strained than **73**, co-incident with a shallower bowl as well.^{31,36} Heterogeneous or homogeneous deuteration of **73** affords *exo*-dideuteriocyclopentacorannulene

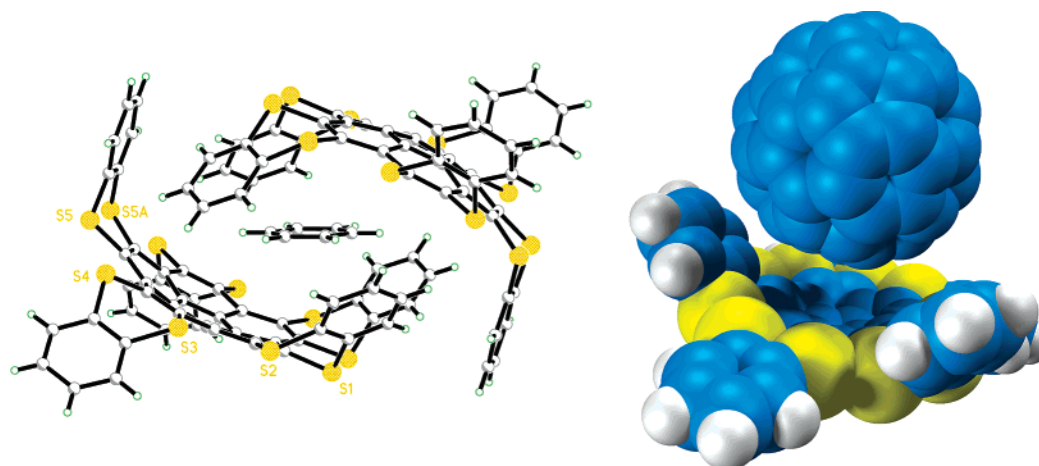
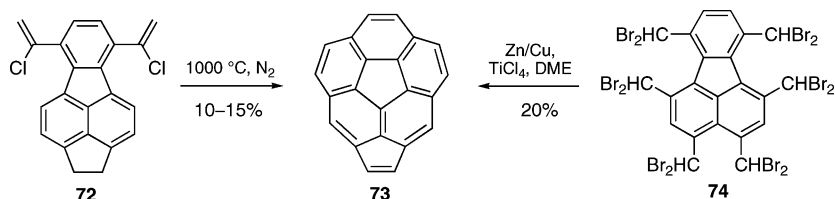
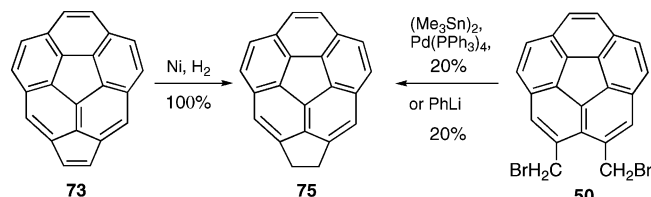


Figure 2. Structure of **71d** in the solid state (left, Reprinted with permission from ref 74. Copyright 2004 Georg Thieme Verlag Stuttgart · New York) and the calculated structure of **71d**:C₆₀ complex (right, Reprinted with permission from ref 49. Copyright 2005 American Chemical Society).

Scheme 17. Synthesis of Cyclopentacorannulene (73)



Scheme 18. Synthesis of Acecorannulene (75)



Scheme 19. peri-Annelated Corannulenes (heterocycles)

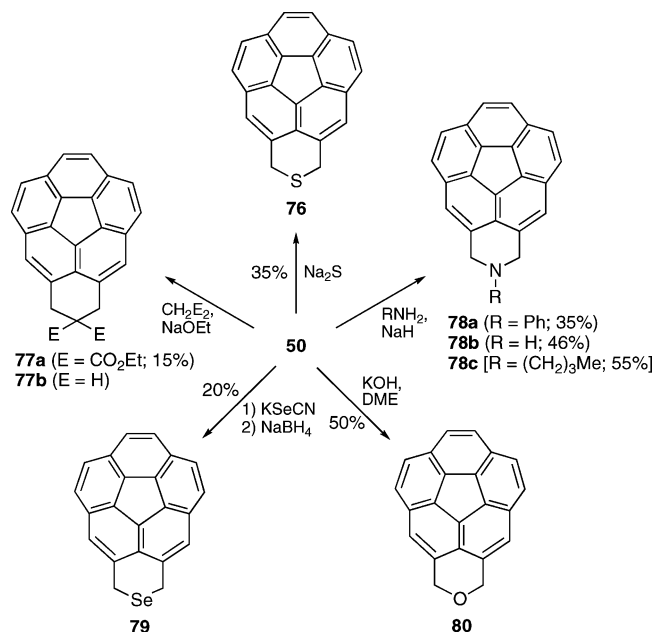


Table 8. $\Delta G_{inv}^{\ddagger}$ and Bowl Depth of (heterocyclic) *peri*-Annelated Corannulenes^{31,35,50,53}

compd.	MP2/cc-pVDZ (sp)		RHF/cc-pVDZ		B3LYP/cc-pVDZ	
	exp. $\Delta G_{inv}^{\ddagger a}$	$\Delta G_{inv}^{\ddagger a}$	$\Delta G_{inv}^{\ddagger a}$	bowl depth ^b	$\Delta G_{inv}^{\ddagger a}$	bowl depth ^b
73		30.9	29.2	1.05	27.7	1.08
75		28.9	26.6	1.04	25.6	1.07
75-D2	27.7					
76	13.9	14.5	12.1	0.863	11.8	0.898
77a	15.5					
77b		15.7	13.8	0.890	13.4	0.928
78a	16.7					
78b	16.1	16.4	14.3	0.903	13.9	0.935
78c	16.6					
79	13.0					
80	17.3	16.9	14.8	0.914	14.7	0.947

^a Units: kcal/mol. ^b Units: Å.

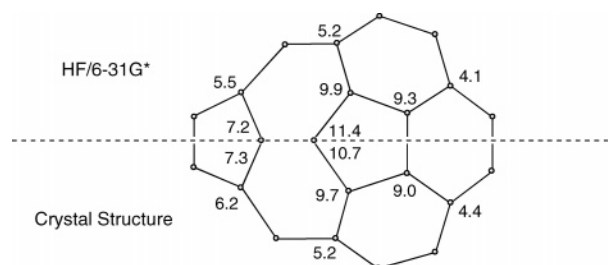


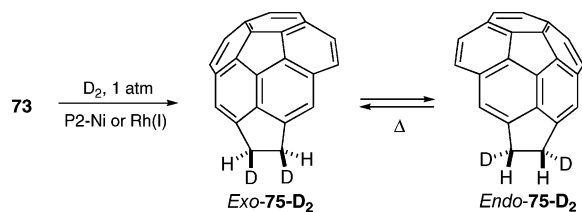
Figure 3. POAV pyramidalization angles for cyclopentacorannulene (**73**).

75-D₂. By following the chemical equilibration at elevated temperatures, a value of $\Delta G_{inv}^{\ddagger} = \text{ca. } 27.6 \text{ kcal/mol}$ was determined.

$\Delta G_{inv}^{\ddagger}$ for (heterocyclic) *peri*-annelated corannulenes depends on the bridging groups. The methylene carbon–heteroatom bond length shortens along the series Se > S > C > N > O and the ring size contracts. This strained

(*exo*-**75-D₂**) with the *exo* specificity (Scheme 20).³⁵ The proton spectra of *exo*-**75-D₂** shows no change on standing at room temperature for several days. Heating the sample causes bowl-to-bowl inversion between *exo*-**75-D₂** and *endo*-

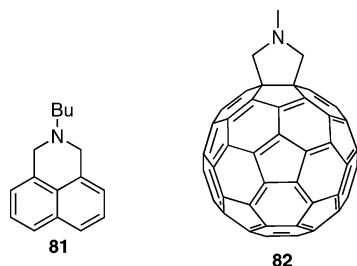
Scheme 20. Synthesis of *exo*-Dideuteriocyclopentacorannulene (*exo*-75-D₂)



annulation leads to a slight increase in bowl depth, but due to the high sensitivity of the inversion barrier to bowl depth there is a significant increase of $\Delta G_{\text{inv}}^{\ddagger}$. Therefore, $\Delta G_{\text{inv}}^{\ddagger}$ for the heterocyclic *peri*-annulated corannulenes follows the sequence **78** > **80** > **76** > **79** (Table 8).³¹ The nitrogen-substituted series **78** was studied in greater detail.⁵³ *N*-Phenyl- and *N*-butyl-substituted 2,3-dihydro-1*H*-corannuleno[2,3-*cd*]-pyridine, **78a** and **78c**, respectively, display $\Delta G_{\text{inv}}^{\ddagger}$ at about 16.5 kcal/mol, slightly higher than that of the NH derivative **78b** (16.1 kcal/mol).

It was also found that the basicity of compound **78c** in CDCl₃ is on par with that of amine **81** (Chart 3) or

Chart 3



morpholine (*pK_a* 7.5) but significantly lower than tribenzylamine (*pK_a* 8.3) and triethylamine (*pK_a* 10.7).⁵³ For comparison, dihydro-*N*-methylfullereno-C₆₀-pyrrole **82** exhibits an even lower basicity like that of *N,N*-dimethylaniline (*pK_a* 5.1). Although the absolute *pK_a* values for **78c** and **82** are solvent dependent, two hypotheses for the basicity trends persist: (1) the fullerene-C₆₀ annellation through the *n*- π interaction results in a much stronger electron-withdrawing effect than the rim annellation on corannulene or (2) the steric bulk of the C₆₀ is more effective in disrupting the solvation shell of the amine. Indeed, the UV and fluorescence spectra

Scheme 21. Synthesis of Dibenzo[*a,g*]corannulene (86**)**

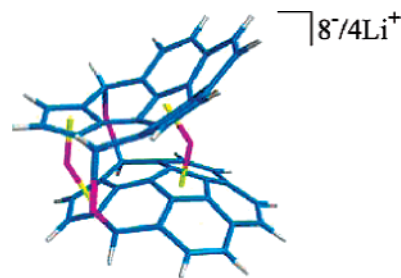
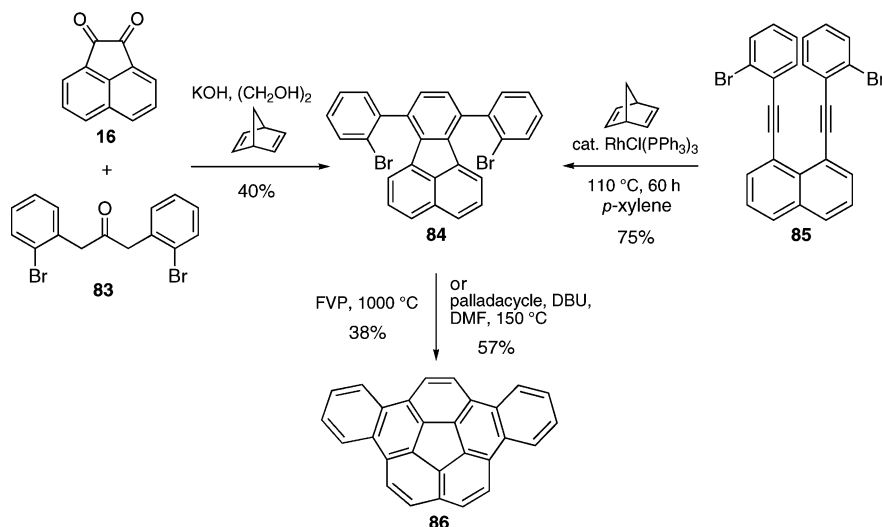


Figure 4. Proposed structure for the reductive coordinative dimer $73^{4-} \cdot 2\text{Li}^+ \cdot 73^{4-} / 6\text{Li}^+$. Reprinted with permission from ref 55. Copyright 2006 American Chemical Society.

of **78b** and 2,3-dimethylcorannulene are essentially identical, indicating that no strong *n*- π mixing is present in either the ground or the excited state. The UV spectrum of **82** shows that the main electronic features of C₆₀ remain and a new absorption band appears.⁵⁴

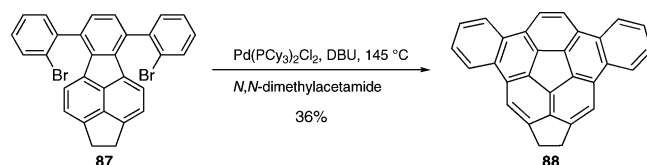
Like corannulene, reduction of cyclopentacorannulene (**73**) with lithium in THF-*d*₈ affords dianion $73^{2-} / 2\text{Li}^+$ and tetraanion $73^{4-} / 4\text{Li}^+$, respectively.⁵⁵ However, tetraanion $73^{4-} / 4\text{Li}^+$ is unlike corannulene to form a sandwich structure, such as $1^{4-} / 4\text{Li}^+ / 1^{4-} / 4\text{Li}^+$. According to NMR and computational studies, the tetraanion of **73** should be a Li⁺-coordinated dimer with a structure $73^{4-} \cdot 2\text{Li}^+ \cdot 73^{4-} / 6\text{Li}^+$ (Figure 4), and the two molecules of **73** point toward different directions. Reduction of **73** with potassium stops at the stage of the trianion radical.

2.4. Dibenzocorannulenes

2.4.1. Synthesis

Dibenzo[*a,g*]corannulene (**86**) is accessible from 7,10-di-(2-bromophenyl)fluoranthene (**84**) by an intramolecular palladium-catalyzed arylation reaction (Scheme 21).¹³ In that report, Scott and co-workers tested various palladium catalysts, bases, and reaction conditions and found the best results to be the combination of palladacycle/DBU/DMF at 150 °C with 57% yield. The FVP technique at 1000 °C can also convert **84** to the desired molecule **86** in modest yield (38%).⁵⁶ The key intermediate **84** is prepared from acenaphthenequinone **16**, ketone **83**, and NBD by a Knoevenagel condensation and a subsequent Diels–Alder reaction in a

Scheme 22. Synthesis of 1,2-Dihydrocyclopenta[*b,c*]dibenzo[*g,m*]corannulene (**88**)



40% yield. Recently, a new synthetic method has been reported to prepare 7,10-disubstituted fluoranthenes, including **84**, from 1,8-bis(ethynyl)naphthalenes and NBD in good to excellent yields by a formal [(2 + 2) + 2] cycloaddition.⁵⁷

Similar to the synthesis of dibenzo[*a,g*]corannulene (**86**), preparation of 1,2-dihydrocyclopenta[*b,c*]dibenzo[*g,m*]corannulene (**88**) has been reported by Sygula et al. (Scheme 22).⁵⁸ The key intermediate **87** is accessible from diketopyracylene, ketone **83**, and NBD, like **84**. Palladium-catalyzed cyclodehydrohalogenation of **87** affords product **88** in 36% yield.

Tetraiodide **62** provides an alternative way to prepare substituted dibenzo[*a,g*]corannulenes. Reaction of **62** and methyl acrylate in the presence of palladium catalyst generates the tetraene **89**, in which both sets of vicinal dienes undergo 6π cyclizations and sequent dehydrogenations to produce dibenzo[*a,g*]corannulene derivative **90a** (Scheme 23).⁵⁹ Under the same conditions, **62** and styrene give **90b** in a one-pot operation.

2.4.2. Structures and Properties

As expected, the X-ray crystal structure of **88** in the solid state exhibits significant curvature, and the POAV pyramidalization angles of the carbon atoms in the central five-membered ring are found to be 10.7°, 10°, 9.6°, 8.7°, and 8.4°. The bowl depth of **88** is 1.033 Å.⁵⁸ On the basis of variable-temperature ¹H NMR experiments and computations at the Becke3LYP/6-31G**//Becke3LYP/3-21G level, $\Delta G_{\text{inv}}^{\ddagger}$ for **88** is estimated as 23.5–23.6 kcal/mol, which is much smaller than that of acecorannulene (**75**, 27.6 kcal/mol).

2.5. Indenocorannulenes

2.5.1. Synthesis

Indeno[1,2,3]annulation of polycyclic aromatic hydrocarbons by a new Suzuki–Heck-type coupling cascade has been developed by de Meijere and co-workers.⁶⁰ This synthetic method easily provides the extension of an aryl functional group with a junction of a five-membered ring in a single synthetic step. Nonsubstituted indenocorannulene **92** has been also prepared in 40% yield by the same method (Scheme 24).

Recently, synthesis of fluoranthene derivatives from 1,8-bis(arylethynyl)naphthalenes and alkynes by a new formal [(2 + 2) + 2] cycloaddition was reported.^{20,57} This successful method was also applied to the preparation of indenocorannulenes **95**.²⁰ The key starting materials 2,3-diethynylcoranu-

lene **94** are accessible from the corresponding 2,3-dichlorocorannulene derivatives **22/31** and trimethyltin-substituted alkynes; several derivatives could be synthesized (Scheme 25). Indenocorannulenes **95** are generated from reaction of diynes **94** and alkynes **19**. It has been observed that the substituents R³ in diynes **94** and R⁴ and R⁵ in alkynes **19** play important roles in this formal [(2 + 2) + 2] cycloaddition (Table 9). Initial studies suggest that alkyl functional groups at the R³ position give lower chemical yields than aryl moieties.

2.5.2. Structures and Properties

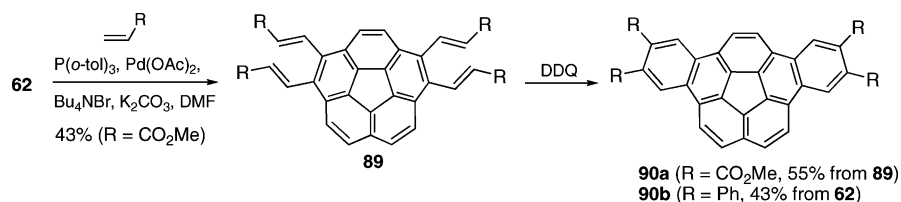
The crystal structure of **95g** is the first example within the indenocorannulene family.²⁰ Curvature and bowl depth are two characteristic features of molecular bowls. The bowl depth in **95g** as gauged from the distance between hub and rim planes is ca. 1.04 (exptl) and 1.07 Å (calcd). The POAV pyramidalization angles for the carbon atoms of the hub ring are 8.8°, 9.8°, and 10.8° (exptl) vs 9.0°, 9.9°, and 11.0° (calcd), respectively (Figure 5); however, the benzo ring adopts a more flat conformation (POAV = 0.1°, 4.7°, and 6.4°). Determination of the coalescence temperature for **95b** is limited by temperature specifications on the NMR instrument. Energetic computation of $\Delta G_{\text{inv}}^{\ddagger}$ for the nonsubstituted indenocorannulene (**92**) via MP2/cc-pVDZ//B3LYP/cc-pVDZ is estimated as 29.8 kcal/mol.

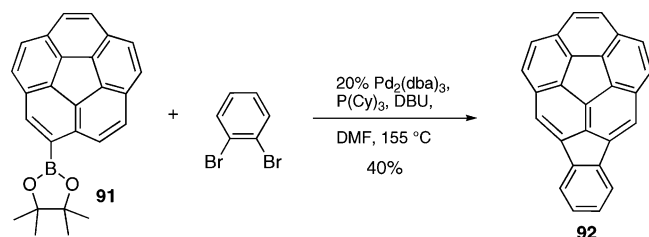
Rabinovitz and co-workers reported that indenocorannulene tetraanion **92⁴⁻/4K⁺** could be formed by a four-step reductive process with potassium (Scheme 26).⁶¹ Each reduced species displays a different color. The first and third stages of reduction give dianion **96²⁻/2K⁺** and hexaanion **96⁶⁻/6K⁺**, which are accessible from **92⁻/K⁺** and the trianion radical (not shown), respectively, by a radical dimerization. As with dibenzofulvene radical anion, the maximum radical density should be generated at the C3 position of the trianion radical **92³⁻/3K⁺** that then dimerizes through coupling at C3 to form **96⁶⁻/6K⁺**. DFT calculations (B3LYP/6-311G**) also predict a high spin density for the odd electron at the C3 carbon atoms. Furthermore, the second and fourth stages of reduction give dianions **92²⁻/2K⁺** and tetraanion **92⁴⁻/4K⁺** by cleavage of the σ bond. Publication of these unusual properties constitutes the first report that a large nonplanar PAH can exhibit multiple dimerization/bond-cleavage stages. Additionally, a significant counterion effect is observed. Reduction of **92** with lithium gives the cognate dianion **96²⁻/2Li⁺** at reduction stage one and dianion **92²⁻/2Li⁺** at reduction stage two. Further reduction of dianion **92²⁻/2Li⁺** with lithium affords the unstable trianion, but the tetraanion **92⁴⁻/4Li⁺** has not yet been observed.

2.6. Other Corannulene Derivatives

Corannulene Cyclophanes. Siegel and co-workers prepared the first corannulene cyclophane **97** in 1996.¹⁴ Bromination of 2,5-dimethylcorannulene **27a** with *N*-bromosuccinimide affords the key intermediate **53**, which cyclizes to

Scheme 23. Synthesis of Tetrasubstituted Dibenzo[*a,g*]corannulene Derivatives **90**

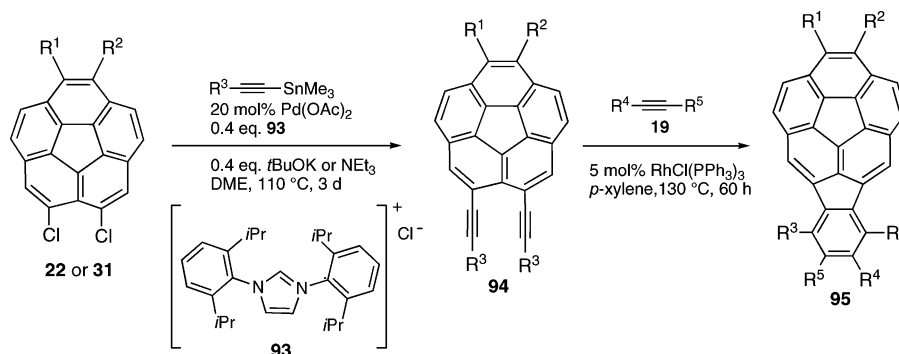
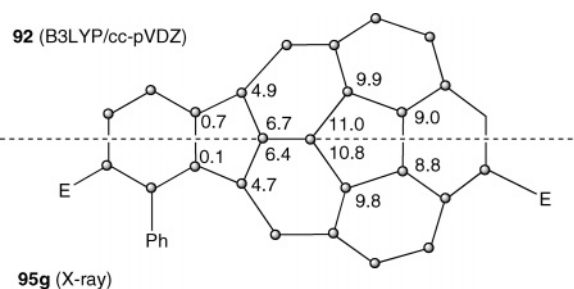
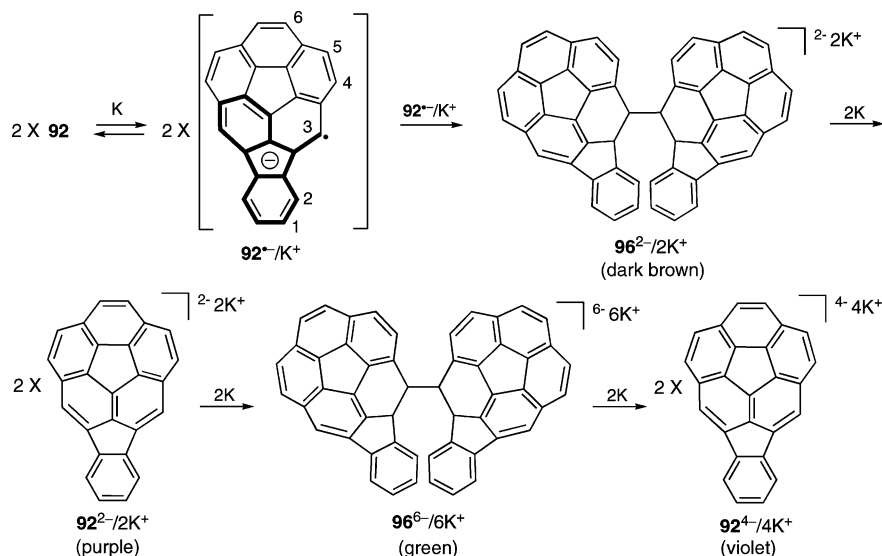


Scheme 24. Synthesis of Indenocorannulenes **92 by a New Suzuki–Heck-type Coupling**

Table 9. Preparation of Highly Substituted Indenocorannulenes **95**

entry	S.M.	R ¹	R ²	R ³	diyne	yield (%)	R ⁴	R ⁵	product	yield (%)
1	22	H	H	Ph	94a	33	Ph	Ph	95a	54
2	22	H	H	Ph	94a		CM ₂ OH	H	95b	60
3	22	H	H	<i>n</i> Pr	94b	34	CH(OEt) ₂	H	95c	14 ^a
4	22	H	H	<i>n</i> Pr	94b		Ph	Ph	95e	42
5	31a	E ^b	E	Ph	94c	65	Ph	Ph	95f	64
6	31a	E	E	Ph	94c		E	E	95g	19
7	31a	E	E	Ph	94c		<i>n</i> Pr	<i>n</i> Pr	95h	57
8	31a	E	E	<i>n</i> Pr	94d	51	Ph	Ph	95i	47
9	31b	Ph	E	Ph	94e	42	Ph	Ph	95j	81

^a **95c** was isolated as an aldehyde and **94b** (69%) was recovered.
^b E = CO₂Me.

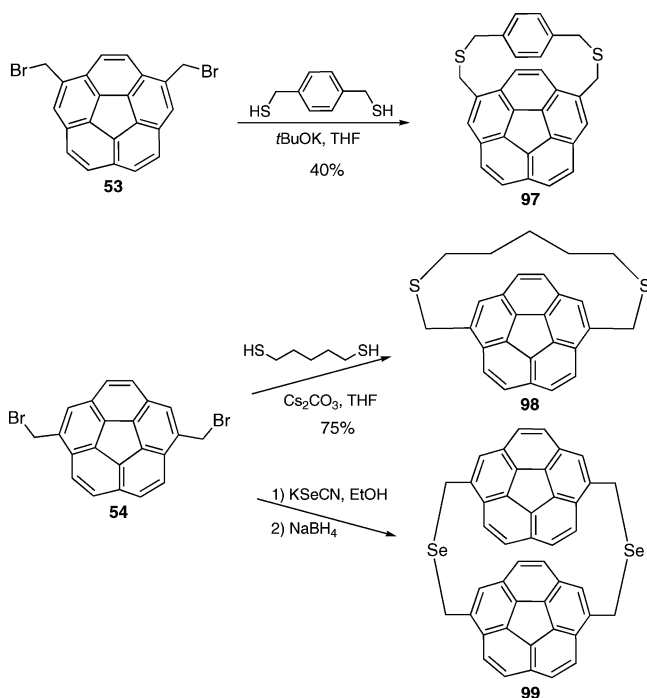
97 upon slow addition to a mixture of 1,4-bis(mercapto-methyl)benzene, potassium *tert*-butoxide, and tetrahydrofuran (Scheme 27). Similarly, 1,5-pentadithiol/1,6-bis(bromo-methyl)corannulene cyclophane (**98**) can be also prepared

Scheme 25. Preparation of Highly Substituted Indenocorannulenes **95 from Diynes **94** and Alkynes **19****

Scheme 26. Reduction Process of Indenocorannulene (92**) with Potassium**

Figure 5. POAV pyramidalization angles for indenocorannulenes.

from **54** and 1,5-pentadithiol in 75% yield.⁶² Synthesis of [3,3]seleno/1,6-dimethylcorannulene cyclophane (**99**), a cyclophane from two corannulenes, was not straightforward. Transformation of **54** to the bis(selenocyno) derivative and subsequent formation of the bis(selenide anion) with NaBH₄ in the presence of additional **54** afford the seleno-bridged dimer **99**, which has poor solubility in most organic solvents. The sulfur analogue of **99** has not yet been prepared.

The calculated bowl depth for **97** in the most stable form agrees well with the experimental bowl depth found in corannulene (0.87 vs 0.89 Å, respectively) and indicates that no significant amount of strain is introduced by forming the cyclophane. Nonetheless, the molecule is conformationally restricted. According to the variable-temperature ¹H NMR study, no coalescence or peak broadening was found at 148 °C.^{14,62} This observation, in conjunction with the large peak separation for the *exo* and *endo* benzene ring signals, sets

Scheme 27. Synthesis of Corannulene Cyclophane 97–99



the minimum limit for the barrier to benzene ring flip at 18 ± 1 kcal/mol. Thus, construction of the cyclophane effectively locks the structure into only one bowl form.

In comparison, the calculated bowl depth of the most stable form of cyclophane **98** (0.96 Å) is significantly increased relative to the calculated bowl depth of free corannulene or **97**.⁶² This increase in bowl depth is associated with an increase of ca. 5 kcal/mol for $\Delta G_{\text{inv}}^{\ddagger}$. Here too the bowl is locked into one form and distorted as folded in a bilaterally symmetric way. The jump-rope motion of the bridge is precluded and from the proton signals along the bridge the ring anisotropy estimated to be similar to that in pyrene, a comparably sized PAH.

Two isomers of **99** are possible, a head-to-tail form **99a** and a head-to-head form **99b**. The former is more stable than the latter by ca. 1.5 kcal/mol.⁶² In the synthesis described above, **99a** is formed predominantly and its structure confirmed by transannular NOE experiments. The juxtaposition of the capping C₂₀ fragments in **99a** is the same as in C₆₀. Looking down the 5-fold axis of C₆₀ or the mirror plane in **99a** one sees that the proximal and distal five-membered rings are *anti* with respect to each other (Figure 6). The calculated bowl depth of **99a** (0.86 Å) is, if anything, slightly flattened with respect to that of corannulene.

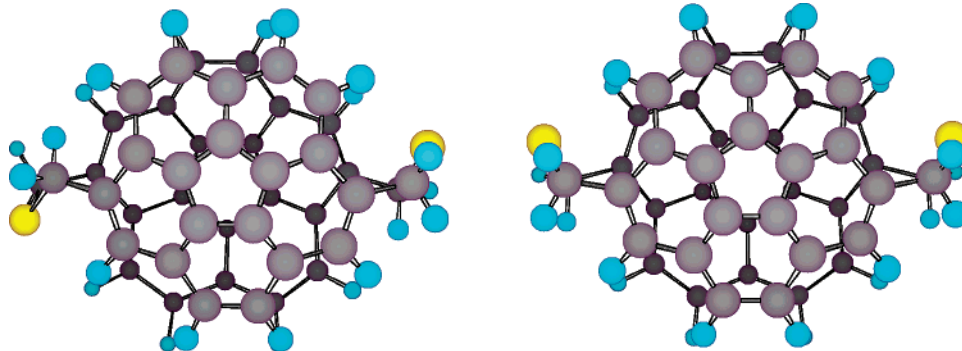


Figure 6. Structures of the head-to-tail and head-to-head isomers **99a** and **99b**. Reprinted with permission from ref 62. Copyright 2001 Elsevier.

Twin Corannulene. The novel twin corannulene **101** is prepared from cyclopentadienone **18** and 1,4-benzoquinone via an intermediate **100** (Scheme 28).⁶³ Diels–Alder reaction of **100** with dimethyl acetylenedicarboxylate and closing four six-membered rings with Method D (Scheme 6) affords designed molecule **101**. Since **101** contains two corannuleny bowl subunits, three conformers, **101A–C**, should exist. Computational calculations (AM1 and Becke3/6-311G**//Becke3/3-21G levels) suggest the energetic stability in the series **101A** > **101C** > **101B** with relatively small energy difference. The room-temperature ¹H NMR spectrum of **101** exhibits only five different signals. Upon cooling, the spectrum becomes complicated, consistent with the presence of multiple conformers. Single-crystal analysis of **101** revealed conformer **101A** in the solid state, and its POAV angles are very similar to corannulene itself.

as-Indaceno[3,2,1,8,7,6,-pqrstuv]picenes and Semibuckminsterfullerene. Shevlin et al. developed a new efficient method to prepare benzo[ghi]fluoranthenes from benzo[g]-phenanthrenes derivatives by palladium-mediated couplings.⁶⁴ This novel method also provides a route to synthesis of *as*-indaceno[3,2,1,8,7,6,-pqrstuv]picenes (**104**). The key starting materials, dichlorobenzo[s]picenes **103a**, are generated from *trans*-2,3-distyrylnaphthalenes **102** by double-photocyclization oxidation in the presence of iodine and propylene oxide (Scheme 29). Palladium-mediated intramolecular cyclizations convert **103** to **104** in high yields.⁶⁵

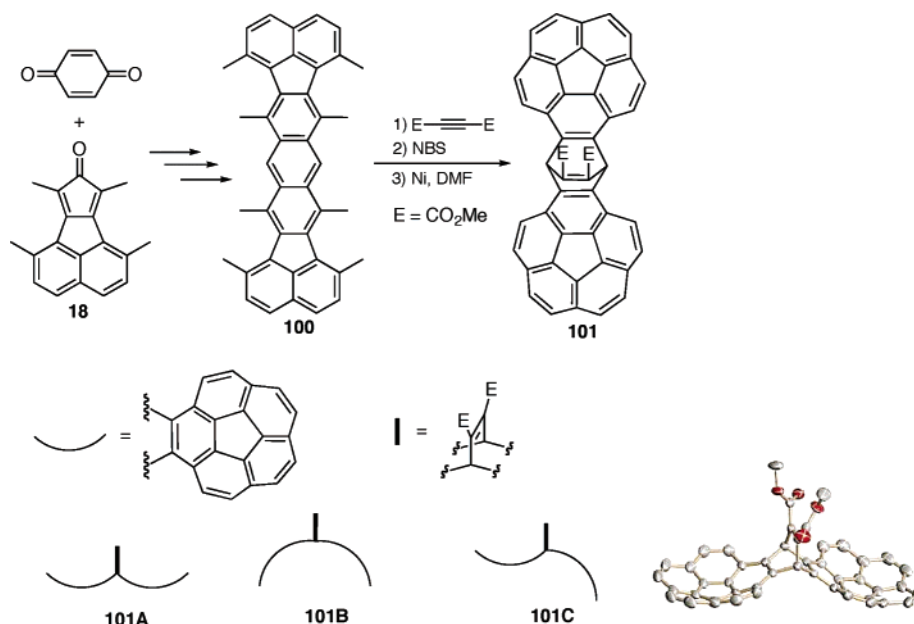
Rabideau and co-workers reported that semibuckminsterfullerenes **106a**¹⁵ and **106b**⁶⁶ could be easily accessible from decabromide **105** via McMurry and carbenoid coupling, respectively (Scheme 30). The four bromine substituents in **106b** can be easily replaced by methyl groups to generate tetramethyl-substituted derivative **106c** in good yield.⁶⁶

Single-crystal X-ray analyses of **104a** and **106c** provide comparisons of curvature for both compounds (Figure 7).^{65,66} Not surprisingly, **104a** is much shallower than **106c**. The local maximum curvature of the former compound is slightly larger than that in corannulene (POAV pyramidalization angles 8.5° vs 8.4°). However, the highest POAV pyramidalization angle of **106c** is at the central carbon atoms with a value of 11.6°, which is almost identical to buckminsterfullerene (11.64°).³³

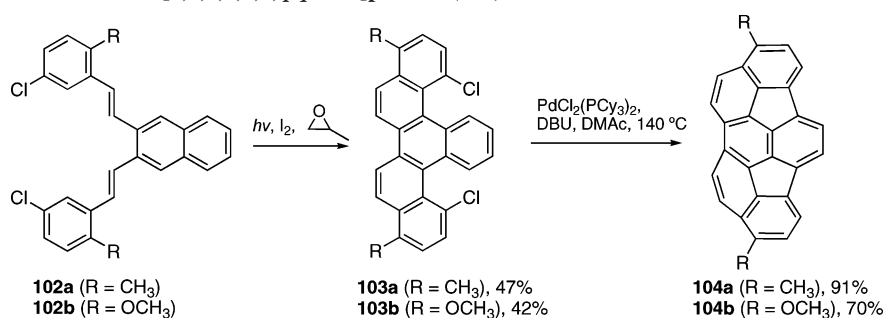
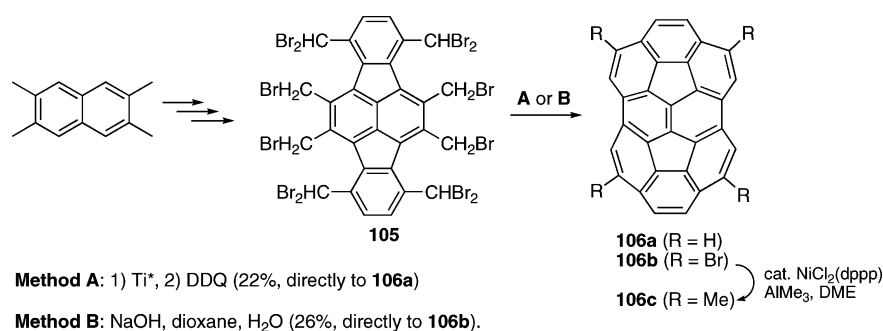
2.7. Complexed Corannulenes and Their Derivatives

2.7.1. η^6 -Complexed Corannulenes and Their Derivatives

2.7.1.1. Synthesis of η^6 -Complexed Corannulenes. Siegel and co-workers reported the first transition-metal-complexed

Scheme 28. Synthesis of Twin Corannulene **101** and its Three Conformers, and the Crystal Structure of **101a**^a

^a The crystal structure of **101a** was provided by Prof. Andrzej Sygula.

Scheme 29. Synthesis of *as*-Indaceno[3,2,1,8,7,6,-*pqrstuv*]picenes (**104**)Scheme 30. Synthesis of Semibuckminsterfullerenes **106**

corannulene **107a**, which is prepared from [Cp**Ru*(MeCN)₃](OTf) and corannulene in CD₂Cl₂ (Scheme 31).⁶⁷ Although

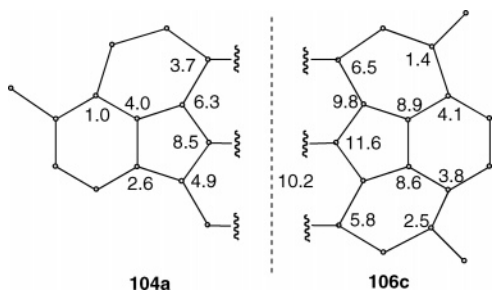


Figure 7. POAV pyramidalization angles of **104a** and **106c** in the crystal.

electron-rich⁶⁸ or electron-deficient⁶⁹ planar arenes form air-stable [Cp**Ru*(η^6 -arene)](OTf) complexes, **107a** is air sensitive in the solid state as well as in solution. The presence of nucleophilic solvents also disrupts Cp**Ru* coordination to corannulene. Addition of acetonitrile to CD₂Cl₂ solutions of isolated **107a** leads to regeneration of **1** and [Cp**Ru*(MeCN)₃](OTf) by arene–nitrile exchange. The iridium analogue **107b** has also been prepared from **1** using {Cp**Ir*[C(O)Me₂]₃}(BF₄) in CD₃NO₂.⁷⁰ As with **107a**, **107b** also shows air sensitivity.

Other η^6 -complexes [(COE)₂Rh(η^6 -C₂₀H₁₀)]PF₆ (**108a**) and [(COE)₂Ir(η^6 -C₂₀H₁₀)]PF₆ (**108b**) are accessible from the unsaturated d⁸ complexes {(COE)₂M[C(O)Me₂]}PF₆ (M = Rh, Ir; COE = cyclooctene) with an equimolar amount of

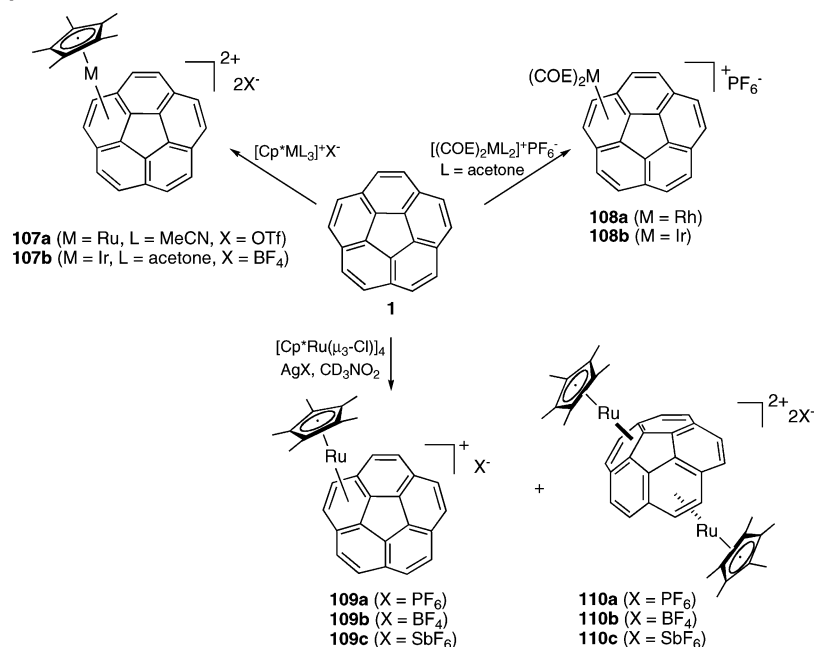
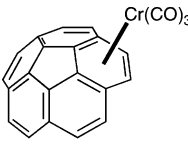
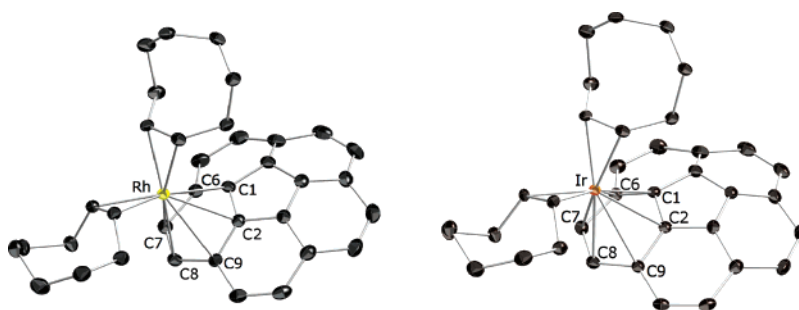
Scheme 31. Synthesis of η^6 -Complexed Corannulenes

Table 10. Calculated Cr–Arene Bond Energies (kcal/mol)

	compound	6-31G*	6-31G*/LanL2DZ	cc-pVDZ
 exo-111	endo-111	51.9	42.3	44.9
	exo-111	57.4	47.3	50.5
	(η^6 -C ₆ H ₆)Cr(CO) ₃ ^a	64.5	54.0	57.7

^a Experimental value: 53 kcal/mol.

Figure 8. Crystal structures of *exo*-heptamers **108a** (left) and **108b** (right). Reprinted with permission from ref 71. Copyright 2006 American Chemical Society.

corannulene at room temperature.⁷¹ In contrast to complexes **107**, these [(COE)₂M]⁺ fragments can undergo chemical transformations while still bound to corannulene.

Recently, Angelici and co-workers provided a new method to prepare stable ruthenium-complexed corannulenes **109** and **110** and analyzed their structures in the solid state (Scheme 31).⁷² Selective formation of mono- and dimetallated corannulenes **109** and **110**, respectively, depends on the ratio of corannulene and [Cp*Ru]⁺, which is generated from [(Cp*Ru(μ₃-Cl))₄] and silver salts. Complexes **109** can be generated in excellent yields when the ratio of corannulene to [Cp*Ru]⁺ is 4:1. However, the ratio can be modified to 1:2 to obtain complexes **110**.

Several groups have attempted to prepare (η^6 -C₂₀H₁₀)M(CO)₃ (M = Cr, Mo, W) complexes; however, to date, none have been successful.⁷³ DFT calculations for (η^6 -C₂₀H₁₀)-

Cr(CO)₃ (**111**) suggest that *exo*-**111** is more stable than its *endo* isomer and the (η^6 -C₂₀H₁₀)-Cr linkage of the former complex is only a few kcal/mol weaker than the corresponding bond in (η^6 -C₆H₆)Cr(CO)₃ (Table 10). These results imply that failures in syntheses arise from kinetic, not thermodynamic, problems.

2.7.1.2. Structures and Properties. Metal coordination can occur on the convex (*exo* isomer) or concave bowl face (*endo* isomer). Computations on the **107a** analogue [CpRu(η^6 -corannulene)]⁺ and **109c** predict the *exo* isomer to be more stable than the *endo* isomer. Actually, in the crystal structures of **108** (Figure 8)⁷¹ and **109c**,⁷² all metal fragments are η^6 -coordinated to the *exo* side of corannulene.

Another interesting feature, revealed by the crystal structures of **108**, **109**, and **110**, is that the formally η^6 -bonded ring has a shallow boat geometry. In **109c**, the POAV angles

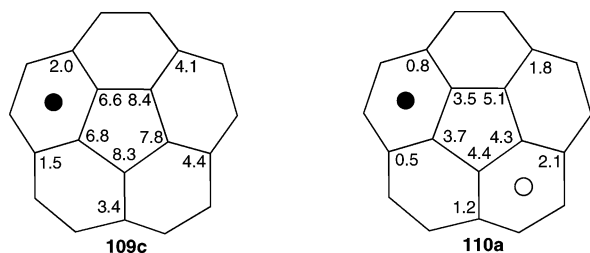


Figure 9. POAV for stable mono- and diruthenium corannulene complexes **109** and **110**

of two core carbons bonded to Ru are slightly smaller than those of the other three carbons and also of free corannulene.⁷² This reduction in POAV upon binding indicates that coordination of the Ru cation to corannulene makes the bowl slightly flatter. Additionally, the molecular packing of **109c** presents the corannulene ligands of the $[\text{Cp}^*\text{Ru}(\eta^6\text{-C}_{20}\text{H}_{10})]$ cation with their concave faces directed toward each other. The shortest intermolecular carbon-to-carbon distance between two corannulene ligands is ca. 3.4 Å.

The crystal structure of $[(\text{Cp}^*\text{Ru})_2(\mu^2\text{-}\eta^6, \eta^6\text{-C}_{10}\text{H}_{20})][\text{PF}_6]_2$ (**110a**) reveals that one unit of $[\text{Cp}^*\text{Ru}]^+$ binds to the convex and the other to the concave side of the corannulene bowl (Figure 9).⁷⁴ In the crystal investigation of **110a**, POAV angles of either the central five-membered ring or the outer six-membered ring are dramatically smaller than that of free corannulene and the corannulene bowl becomes much flatter. The curvature of the corannulene bowl in **110a** is reduced to approximately one-half of the curvature of corannulene and the six-membered ring bonded to the convex $[\text{Cp}^*\text{Ru}]^+$ unit is flatter than that to the concave $[\text{Cp}^*\text{Ru}]^+$ unit. This distortion essentially blurs the distinction between convex and concave complexation.

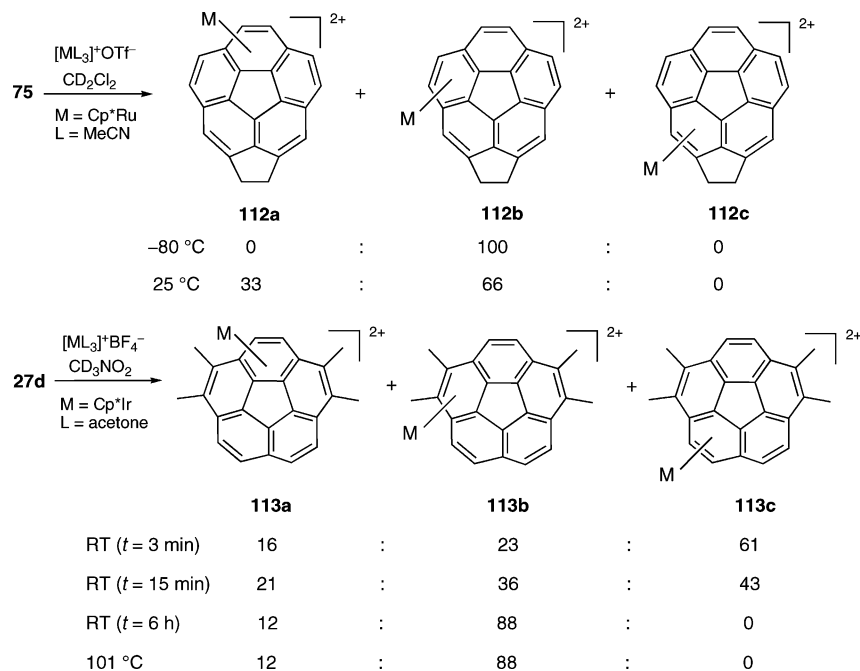
The ^1H NMR spectrum of **108a** displays broad signals in the aromatic region at 25 °C. When the spectra were recorded at lower temperature (0 °C), distinct signals for all of the protons of corannulene were obtained. These data indicate that migration of the $[(\text{COE})_2\text{Rh}]^+$ fragment over the rings of corannulene takes place. The precise mechanism of the

inter-ring movement of the $[(\text{COE})_2\text{Rh}]^+$ fragment remains open.

Obvious inter-ring movements of metal fragments are also displayed on complexed acecorannulene and 1,2,5,6-tetramethylcorannulene. Monitoring the reaction of acecorannulene (**75**) with $[\text{Cp}^*\text{Ru}(\text{MeCN})_3](\text{OTf})$ in CD_2Cl_2 at room temperature reveals that initial formation of isomer **112b** rapidly evolves to an equilibrating mixture of the two isomers **112a** and **112b** in a ratio of 1:2 within 2 h (Scheme 32).⁷⁵ In order to follow the migration process of the ruthenium moiety more closely, the same reaction was conducted at -80 °C, wherein **112b** forms but no isomerization ensues even after 7 h. Upon warming to room temperature, the ratio of **112a** and **112b** stabilizes at 1:2 within 1 h. Computations with the B3LYP/GEN (MP2/Gen/B3LYP/GEN) basis set for the six complexes of **112**, but using Cp instead of Cp^* , indicate that all *exo* isomeric complexes are energetically favored over the respective *endo* complexes and moreover binding to the sites of lowest curvature leads to a more stable complex. The stability of the three *exo* isomeric complexes with the Cp^*Ru^+ follows the series **112b** \approx **112a** > **112c**.

Reaction of **27d** with $\{\text{Cp}^*\text{Ir}[\text{acetone}_2]_3\}(\text{BF}_4)$ in CD_3NO_2 at room temperature after 3 min gives a mixture of three isomers **113a**, **113b**, and **113c** in the ratio 16:23:61 (Scheme 32).⁷⁰ After a long period (6 h), complex **113c** disappears and the ratio between **113a** and **113b** becomes to 12:88, which does not change, even over 1 month. This value can be more readily reached when the reaction for the preparation of complexes **113** is conducted at 101 °C instead of at room temperature. Treatment of the mixture **113a** and **113b** (12:88) with excess benzene and acetone in CD_3NO_2 at room temperature results in complete substitution of **27d** by benzene within 6 h and by acetone within 4 h. It is also found that the disappearance of isomer **113a** is faster than **113b**. The combined results from the above research agree that an alkylated arene in $[\text{Cp}^*\text{Ir}(\eta^6\text{-arene})](\text{BF}_4)_2$ leads to a more stable complex. Thus, complex **113b** is more stable than the other two isomers.

Scheme 32. η^6 -Complexed Corannulene and Acecorannulene Derivatives **112** and **113**



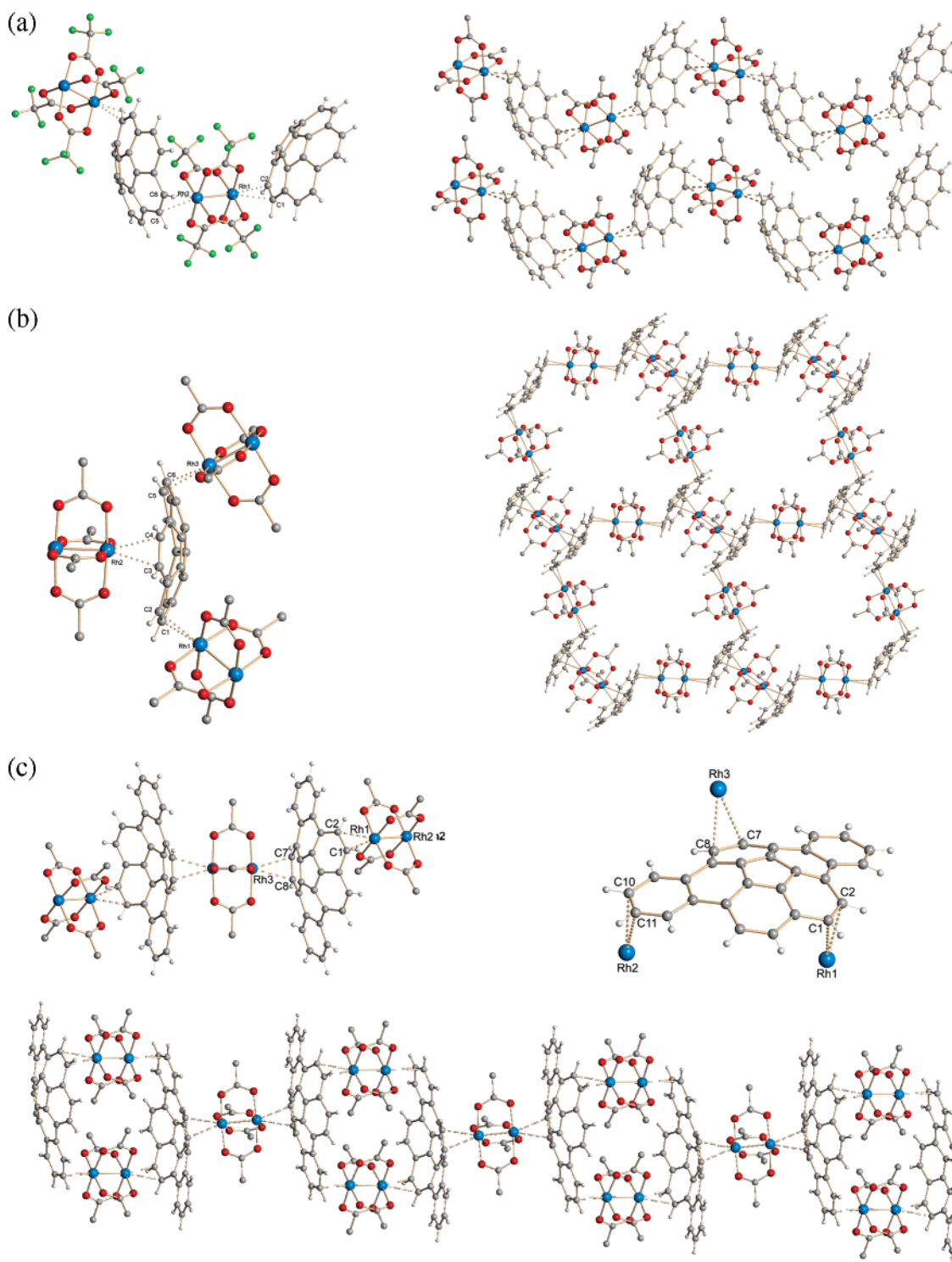


Figure 10. (a) Fragment and crystal packing of **114a** (Reprinted with permission from ref 76. Copyright 2003 Wiley-VCH). (b) Fragment and crystal packing of **114b** (Reprinted with permission from ref 76. Copyright 2003 Wiley-VCH). (c) Fragment and crystal packing of tridentate $\eta^2:\eta^2:\eta^2$ -complex **115** (Reprinted with permission from ref 77. Copyright 2005 American Chemical Society).

2.7.2. η^2 -Complexed Corannulenes and Their Derivatives

Petrukhina et al. prepared the rhodium-complexed corannulene **114** and -dibenzo[*a,g*]corannulene **115** (Figure 10).⁷⁶ These compounds are synthesized from $[\text{Rh}_2(\text{O}_2\text{CCF}_3)_4]$ and the corresponding molecular bowls at 160 °C in a solvent-free environment. The mixture of corannulene and $[\text{Rh}_2(\text{O}_2\text{CCF}_3)_4]$ in the ratio ca. 2:1 favors formation of complex **114a** with composition $\{[\text{Rh}_2(\text{O}_2\text{CCF}_3)_4] \cdot (\text{C}_{20}\text{H}_{10})\}$. On the other hand, as the ratio is changed to ca. 1:3, another isomer **114b**

with the form $\{[\text{Rh}_2(\text{O}_2\text{CCF}_3)_4]_3 \cdot (\text{C}_{20}\text{H}_{10})_2\}$ can be obtained. A similar synthetic procedure to that used to prepare **114**, but substituting dibenzo[*a,g*]corannulene (**86**) for **1**, led to only one isomeric form of $\{[\text{Rh}_2(\text{O}_2\text{CCF}_3)_4]_3 \cdot (\text{C}_{28}\text{H}_{14})_2\}$ (**115**).⁷⁷

A X-ray single-crystal diffraction study of compound **114a** reveals a packing pattern akin to polymeric frieze or so-called one-dimensional (1D) polymer. In the $[\text{Rh}_2(\text{O}_2\text{CCF}_3)_4]$ unit, one Rh coordinates to the convex (*exo*) side of a corannulene

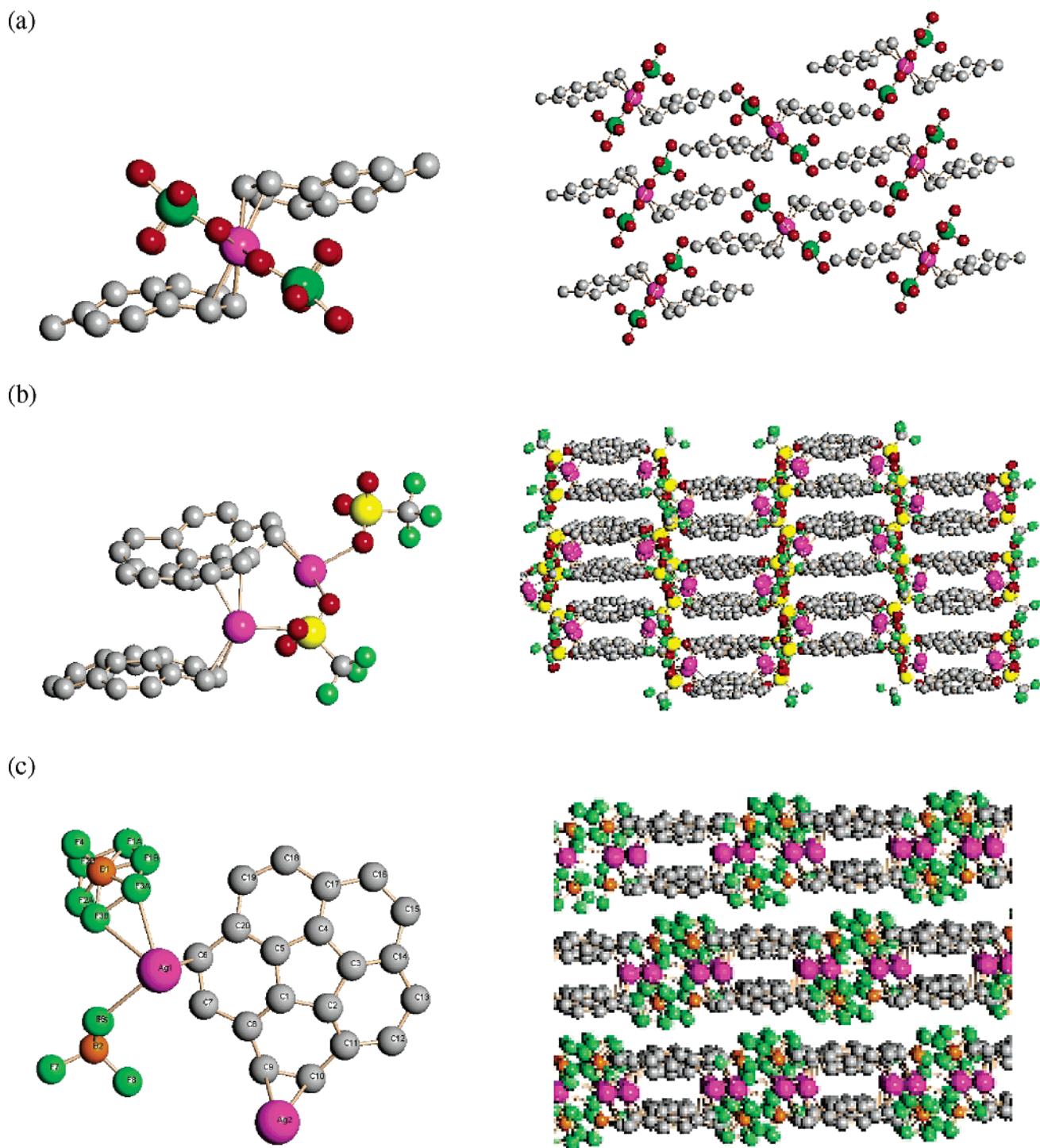


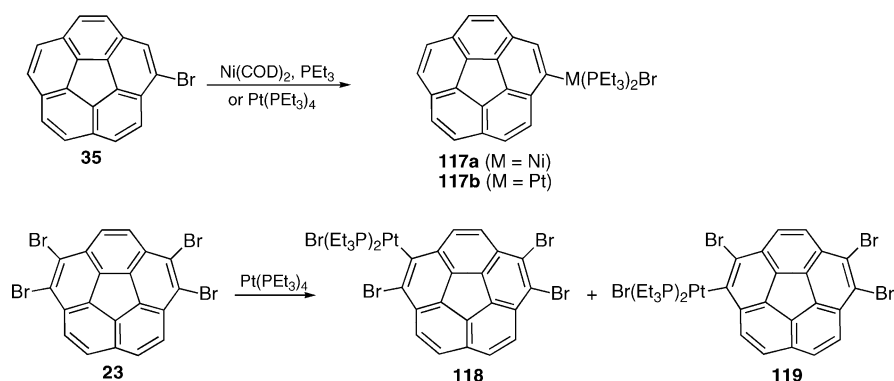
Figure 11. Fragment and crystal packing of silver(I)-complexed corannulenes: (a) $[\text{Ag}(\text{C}_{20}\text{H}_{10})](\text{ClO}_4)$, (b) $[\text{Ag}(\text{C}_{20}\text{H}_{10})](\text{OTf})$, and (c) $[\text{Ag}_2(\text{C}_{20}\text{H}_{10})](\text{BF}_4)_2$. Reprinted from ref 78 (copyright 2005) by permission of the Royal Society of Chemistry.

and the other binds to the concave (*endo*) side of the next corannulene [(a) in Figure 10]. Both Rh centers interact with the rim C=C bonds of **1** in η^2 -coordination mode.

In contrast, **114b** represents an infinite 2D network with a repeating pattern of six $[\text{Rh}_2(\text{O}_2\text{CCF}_3)_4]$ units and six corannulene molecules. Each corannulene provides three η^2 -coordination positions for Rh centers: two on the convex (*exo*) surface and one the concave (*endo*) surface [(b) in Figure 10]. Comparing the geometry of the corannulene fragment in **114b** with free corannulene, one finds that the bond lengths of the coordinated rim C=C bonds of the ligated corannulene are only slightly elongated (0.009 Å in

114a and 0.018 Å in **114b**), and other geometric features of the ligated corannulene remain very similar to the parent structure. The bowl depths of **114a** and **114b** are 0.87 and 0.86 Å, respectively, and suggest that the metal–corannulene interaction is very weak or does not significantly perturb the structure of corannulene. DFT calculations predict that coordination of $[\text{Rh}_2(\text{O}_2\text{CCF}_3)_4]$ to the concave surface of corannulene is only ca. 2 kcal/mol more stable than that to the convex surface.

The crystal packing of **115** forms a frieze or 1D polymer [(c) in Figure 10].⁷⁷ Three Rh η^2 -coordination positions are possible in **86**. The average *exo* Rh–C bond distance is

Scheme 33. Metal σ -Bonded Corannulene Derivatives

slightly longer than those of the two endo Rh–C bonds. Although the C–C bond distances of **86** in **115** shows no significant difference to free **86**, the result of binding three Rh(II) centers to the same unit of **86** flattens the bowl from 0.83 to 0.77 Å.

Reaction of corannulene with different silver(I) salts, e.g., AgClO₄, AgOTf, and AgBF₄, affords various corannulene complexes according to single-crystal structures analyses. The reaction mixture of corannulene and silver(I) salt is used in a ratio 1:1, but the crystal packing motifs depend on the counteranion.⁷⁸ Complex **116a** ([Ag(C₂₀H₁₀)]ClO₄) reveals a 1D polymer with double-layer connectivity (Figure 11). These polymers are packed into a zigzag pattern to minimize the free space. Each corannulene moiety is coordinated to two silver atoms through neighboring rim bonds.

In contrast, crystals of complex **116b** ([Ag(C₂₀H₁₀)]OTf) display two unique silver environments in the solid-state packing. One corannulene ligand is coordinated to two silver atoms through neighboring rim bonds, and the second corannulene ligand is coordinated to two silver atoms through the 1,2- and 5,6-positions. Furthermore, complex **116b** forms wave-like sheets, with each sheet stacked directly atop on another.

Yet different again from complex **116b**, complex **116c** [Ag₂(C₂₀H₁₀)](BF₄)₂ contains two unique silver cations and two unique tetrafluoroborate anions but only one unique corannulene moiety. The corannulene ligand is coordinated to four silver atoms through four of the five rim bonds. Three of these contacts can be described as η^2 bonds and the fourth as an η^1 -bond. The packing pattern of complex **116c** constitutes a nearly planar sheet with successive sheets stacked one atop another. In all three complexes, no statistically relevant deviation in the corannulene C–C bond lengths is observed as a consequence of the coordination.

Although η^2 -Pt(0)-complexed corannulene has not been yet prepared, Sakaki and co-workers predicted that Pt(PH₃)₂-(C₂₀H₁₀) can be synthesized as a stable species.⁷⁹ Theoretical study of this compound indicates that Pt coordinates to corannulene at a rim position with η^2 mode and that the binding energy is 24.9 kcal/mol, which is similar to that of Pt(PH₃)₂(C₂H₄).

2.7.3. Metal-Bonded Derivatives of Corannulene

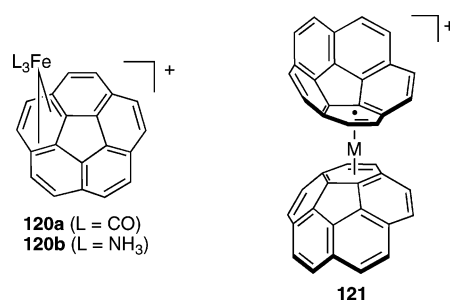
Lee and Sharp reported the first σ -bonded corannulene complexes. Addition of Ni(COD)₂ to a mixture of bromo-corannulene (**35**) and PEt₃ immediately forms complex **117a** (Scheme 33).⁸⁰ The structure of **117a** was confirmed by single-crystal structure analysis. Complex **117b** is also accessible from **35** and Pt(PEt₃)₄. In both complexes, the

metal coordination plane is approximately orthogonal to the corannulene bowl, and it leads two *trans* phosphine ligands with one *exo* and one *endo* to the bowl. Variable-temperature NMR studies indicate $\Delta G^\ddagger_{\text{inv}}$ for **117a** and **117b** is 11.6 and 12.2 kcal/mol, respectively. These values are very close to some simple corannulene derivatives (cf. Table 5). Similarly, treatment of a toluene solution of **23** with 1 equiv of Pt-(PEt₃)₄ from room temperature to 130 °C gives a mixture of **118** and **119**, and the latter regioisomer was isolated as the major product.

2.7.4. η^n -Complexed Corannulenes and Their Derivatives in the Gas Phase

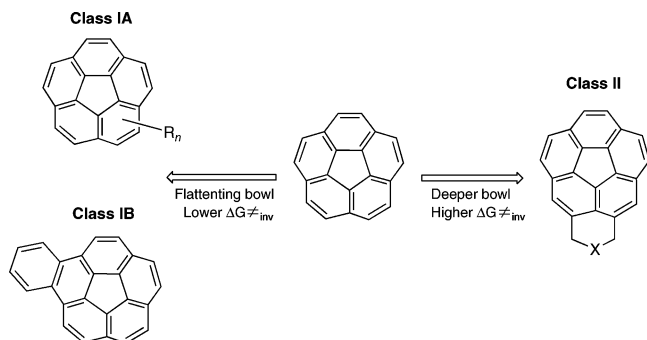
Cariman et al. studied the reactivity of C₂₀H₁₀Fe⁺ in the gas phase with small molecules, i.e., D₂, N₂, CO₂, CH₄, C₂H₂, C₂H₄, SO₂, C₆D₆, NH₃, H₂O, and CO.⁸¹ Complex C₂₀H₁₀Fe⁺ is generated by the association reaction of Fe⁺ with the corannulene vapor in a ratio of about 30:1. More interestingly, reactions of C₂₀H₁₀Fe⁺ with CO and NH₃ generate molecular ions for C₂₀H₁₀Fe(CO)₃⁺ and C₂₀H₁₀Fe(NH₃)₃⁺. Because η^2 -coordinated C₆₀Fe⁺ can add four molecules of CO and NH₃ to form a complete 18-electron ligand field, it is reasonable to propose that coordination of Fe⁺ in **120a** and **120b** takes place at the smaller corannulene curvature in an η^4 mode (Chart 4). However, the relative stabilities of

Chart 4



cationic C₂₀H₁₀Fe⁺ at various binding sites resulting from DFT studies can be given as follows convex- η^6 -site > concave- η^6 -site > convex- η^5 -site > concave- η^5 -site.⁸²

More recently, Ayers et al. reported their study on the reactivity of metal ions and corannulene and the possibility for preparation of multiple metal atom corannulene complexes in the gas phase.⁸³ Gas-phase [M(C₂₀H₁₀)]⁺-molecule complexes are produced by copolymerization of metal ion sources, including Cr, Ti, UOAc, [CpFe(C₆H₆)](PF₆), and corannulene, with 532 nm laser light and detected using a TOF-MS. This procedure cannot provide efficient methods

Scheme 34. Correlations between Structures and Bowl-to-Bowl Inversion Energy


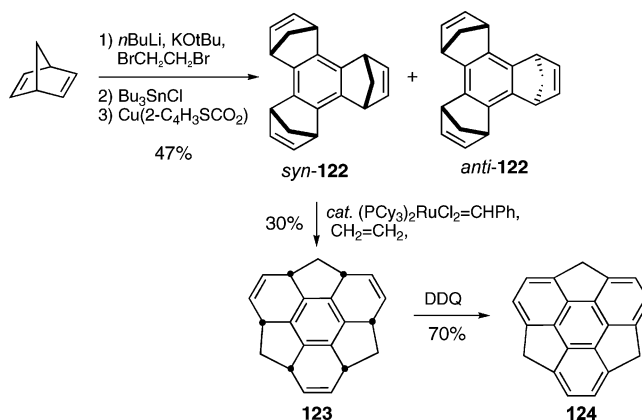
for production of multiple metal atom corannulene complexes or complexes containing more than two corannulene molecules. Cr, Ti, and UOAc efficiently produce mono- and dicorannulene complexes of the form $M(C_{20}H_{10})_n^+$, with $n = 1, 2$. However, metal oxides, TiO^+ and UO^+ , are found to produce monocorannulene complexes $M(C_{20}H_{10})^+$ with high efficiency. Covaporization of $[CpFe(C_6H_6)](PF_6)$ with corannulene yields $Fe(C_{20}H_{10})^+$, $CpFe(C_{20}H_{10})^+$, and $Fe(C_{20}H_{10})_2^+$ but no $(C_6H_6)Fe(C_{20}H_{10})^+$. The binding energy of the iron cation to corannulene (ca. 84 kcal/mol)^{82,83} is suggested to be greater than its binding energy to benzene (ca. 37.8–44.7 kcal/mol)⁸⁴ but less than its binding energy to cyclopentadiene (91 kcal/mol).⁸⁵ Complexes $M(C_{20}H_{10})_2^+$ should be a sandwich structure, and metal ion binds to corannulene on the convex side in one of the outer η^6 ring sites rather than on the η^5 interior site (cf. **121** in Chart 4).

2.8. Correlations between Structures and Bowl-to-Bowl Inversion Energy (ΔG_{inv}^\ddagger)

The correlations between structures and ΔG_{inv}^\ddagger can be simply described as in Scheme 34 with a focus on bowl depth being directly related to the height of the bowl inversion barrier (ΔG_{inv}^\ddagger). Compounds of Class IA and Class IB (with a benzene ring fused to a rim of corannulene), where the bowl is more shallow than that found for **1**, lead in general to a decrease of ΔG_{inv}^\ddagger relative to **1**. In this class, **67c** and metal σ -bonded derivatives of corannulene do not follow this principle. In contrast, compounds of Class II lead in general to an increase of ΔG_{inv}^\ddagger relative to **1**. As the distance between two methylene groups in Class II decreases, the additional ring is more strained in the transition state to bowl inversion, which in part explains the observation that the value of ΔG_{inv}^\ddagger increases. Cyclopentacorannulene (**73**) and acecorannulene (**75**), with a direct connection between the *peri* carbon atoms, have the highest ΔG_{inv}^\ddagger within the simple annelated-corannulene family. The lower values of ΔG_{inv}^\ddagger for 1,2-dihydrocyclopenta[*b,c*]dibenzo[*g,m*]corannulene (**88**) and indenocorannulenes **92** than **73/75** can be also fitted to the principle of Class I, i.e., the shallower bowl gives rise to the lower inversion barrier.

In order to develop a quantitative structure–energy relationship, Siegel and co-workers investigated the correlation between bowl depth and barrier energy for some corannulene derivatives and found that the relationship can be empirically expressed as in eq 1. This simple quartic equation provided a reasonable fit to the experimental results³¹

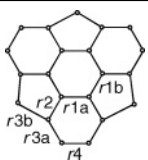
$$[\Delta G_{inv}^\ddagger = (\text{bowl depth}/0.87)^4 \times 11.5 \text{ kcal/mol}] \quad (1)$$

Scheme 35. Synthesis of Sumanene (124)

3. Sumanene

Sumanene (**124**) is another symmetric subunit of C_{60} with a bowl structure when expressed as its parent hydrocarbon ($C_{21}H_{12}$). The FVP conditions are as of yet unknown for obtaining this structure.⁸⁶ Recently, Sakurai et al. provided a new synthetic method to prepare **124** in solution under mild conditions.⁸⁷ Similar to Lawton's synthetic strategy for corannulene, they first constructed the three-dimensional framework using tetrahedral sp^3 carbons and later aromatized the structure oxidatively to obtain the designed product. Trimerization of norbornadiene via an organotin compound affords *syn*- and *anti*-**122** (ratio 1:3) in a total yield of 47% (Scheme 35). Treatment of *syn*-**122** with $Cl_2(PCy_3)_2Ru=CHPh$ under an atmospheric pressure of ethylene gives **123** in 30% yield by a ring-opening metathesis (ROM) and subsequent ring-closing metathesis (RCM) reaction. Finally, **124** can be accessible from **123** in 70% yield by oxidation with DDQ.

Variable-temperature NMR of sumanene **124** in *p*-xylene- d_{10} solution reveals a barrier to inversion ΔG_{inv}^\ddagger of 19.6 kcal/mol. The result suggests that **124** is much more rigid than corannulene. The molecular structure of **124** by X-ray crystal structure analysis indicates significant bond alternation in the hub six-membered ring to give the bond lengths of *r*1a and *r*1b as 1.381 and 1.431 Å, respectively (Table 11).⁸⁸ In

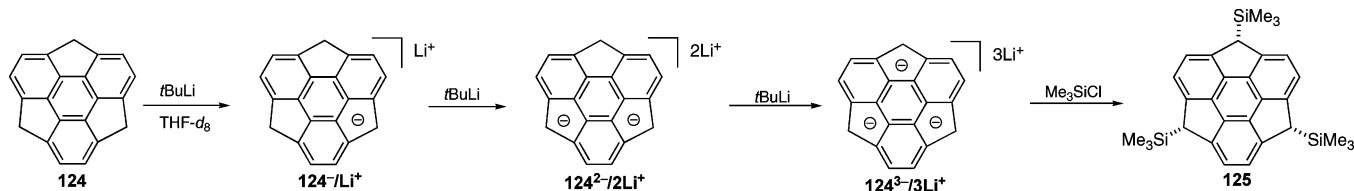
Table 11. Observed and Calculated Bond Lengths of 124

	bond length (Å)	crystal structure	B3LYP/6-31G**
	<i>r</i> 1a	1.381	1.387
	<i>r</i> 1b	1.431	1.433
	<i>r</i> 2	1.396	1.399
	<i>r</i> 3a	1.398	1.400
	<i>r</i> 3b	1.548	1.556
	<i>r</i> 4	1.430	1.432

contrast, the bond lengths in the flank six-membered ring (*r*1a, *r*2, *r*3a) are almost identical except for a significantly elongated rim bond (*r*4). POAV analysis indicates that the hub six carbons are pyramidalized to an extent of 9.0°. The bowl depth is observed as 1.11 Å. Molecule packing of **124** is in a concave–convex fashion to form a column, and every column is present in the same direction. Each layer of the column is stapled in a staggered fashion with a 3-fold axis.

Generation of mono-, di-, and trianions of **124** in THF- d_8 depends on the amounts of *t*BuLi used (Scheme 36).⁸⁸ Furthermore, the difference in chemical shifts between *exo/endo* benzylic protons in **124** is in the series dianion >

Scheme 36. Synthesis of Sumanene Derivative 125



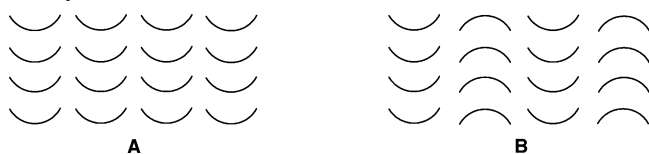
monoanion $>$ free **124**. On addition of 3 equiv of *t*BuLi, the trianion is considered to be generated and excess amounts of Me_3SiCl are introduced to the solution of $124^{3-}/3\text{Li}^+$ to afford the tris(trimethylsilyl) derivative **125** as the sole isomer. The trimethylsilyl group is introduced at the *exo* position with perfect selectivity, probably due to the steric demand. Three benzylic positions of **124** are readily functionalized via the corresponding carbanions to extend bowl-shape compounds.

4. Molecular Packing of Bowls in the Solid State

Controlling the molecular stacking of polynuclear aromatic compounds in their crystal structures is an important topic in supramolecular chemistry.⁸⁹ The π - π interactions of planar aromatics have been well studied and analyzed.⁹⁰ However, not as many crystal structures of bowl-shaped aromatic compounds are reported; therefore, the factors necessary to form the bowl stacking are still not well known. The molecule stacking and alignment of the bowl-shaped aromatic compounds in the solid state affect the dipoles and electronic properties.^{90d}

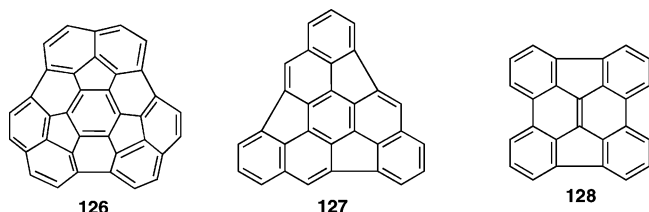
Summarizing the crystal structures of nine different curved aromatic compounds with regard to the possibility of bowl-in-bowl stacking, one can classify them as belonging to three different types (Scheme 37).⁹¹ Type A: bowl-in-bowl stacks

Scheme 37. Schematic Presentations of Open Geodesic Bowl in Crystals



where all columns are oriented toward the same direction resulting in polar crystals. Examples of type A include circumtrindene (**126**, $\text{C}_{36}\text{H}_{12}$, Chart 5)⁸⁹ and trigonal crystals

Chart 5



of hemibuckminsterfullerene (**127**, $\text{C}_{30}\text{H}_{12}$)⁹² and sumanene (**124**).⁸⁸ In principle, the molecular packing of diindenol[1,2,3,4-*diefg*;1,2,3,4-*mnop*]chrysene (**128**, $\text{C}_{26}\text{H}_{12}$)⁹³ and semibuckminsterfullerene (**106c**, $\text{C}_{30}\text{H}_{12}$)⁶⁶ in crystals also belongs to this class. The stack is on the whole pointed in one direction, and the crystals are polar, but within each stack the bowls are alternatively slipped slightly from side to side. Type B: bowl-in-bowl stacks where neighboring columns are oriented toward opposite directions, resulting in apolar

crystals. Examples of type B include orthorhombic crystals of hemibuckminsterfullerene (**127**, $\text{C}_{30}\text{H}_{12}$),⁹² cyclopentacorannulene (**73**, $\text{C}_{22}\text{H}_{10}$),⁵¹ twin corannulene **101**,⁶³ and 4,5,10,11-tetra(methoxycarbonyl)-9,12-diphenylindencorannulene (**95g**).²⁰ Type C (not shown): Any of a number of arrangements devoid of columnar structure, some of which are polar but most not. Examples of type C include corannulene (**1**),³² 1,2-dihydrocyclopenta[*b,c*]dibenzo[*g,m*]corannulene (**88**),⁵⁵ and pentakis(1,4-benzodithio)corannulene (**71d**).⁴⁷

Consideration of the above classifications leads one to some speculations about how one might engineer crystal forms within this family of bowl-shaped polynuclear aromatics. The molecule packing appears to depend on the size of the bowl surface area and the depth of the bowl with larger and deeper favoring types A and B. A large surface area favors types A and B due to strong π - π interactions. As the aromatic molecule becomes smaller and smaller, the molecule packing changes to Type C.

5. Conclusions and Outlook

The synthesis, chemistry, and properties of polynuclear aromatic molecular bowls are very interesting topics. Some of these compounds with strain structures have been prepared in the solution phase. The most important advantages of this synthetic technology rather than that with the FVP synthetic method are tolerances of functional groups and preparations on large scales. These great advances make a reasonable route to synthesize carbon tubes with homogeneous molecular weight distributions. Additionally, modification of the attached functional groups would easily change their physical properties. Unlike planar aromatics, convex and concave surfaces of molecule bowls provide different chemical and physical environments. Control of crystal packing of molecule bowls to form perfect all bowl-bowl stacking in the same direction will be another interesting topic in this field. It will be important for not only basic research in molecule engineering, but also applications in materials science.

6. References

- Beck, A.; Bleicher, M. N.; Crowe, D. W. *Excursions into Mathematics*; Worth: New York, 1969.
- (a) Sygula, A.; Rabideau, P. W. In *Carbon-Rich Compounds: From Molecules to Materials*; Haley, M., Tykwinski, R., Eds.; Wiley-VCH: Weinheim, 2006; p 529. (b) Hirsch, A. *Top. Curr. Chem.* **1999**, *199*, 1. (c) Scott, L. T. *Pure Appl. Chem.* **1996**, *68*, 291. (d) Rabideau, P. W.; Sygula, A. *Acc. Chem. Res.* **1996**, *29*, 235. (e) Terrones, H.; Mackay, A. L. In *The Fullerenes*; Kroto, H. W., Fischer, J. E., Cox, D. E., Eds.; Pergamon: Oxford, 1993; p 113. (f) Seiders, T. J.; Siegel, J. S. *Chem. Br.* **1995**, *31*, 307.
- Kroto, H. W.; Heath, J. R.; O'Brien, S. C.; Curl, R. F.; Smalley, R. E. *Nature* **1985**, *318*, 162.
- Iijima, S. *Nature* **1991**, *354*, 56.
- Dresselhaus, M. D.; Avouris, P. In *Carbon Nanotubes, Synthesis, Structure, Properties, and Applications*; Dresselhaus, M. D., Dresselhaus, R. S., Avouris, P., Eds.; Springer: Heidelberg, 2001; p 1.
- (a) Barth, W. E. Ph.D. Thesis, University of Michigan, Ann Arbor, MI, 1966. (b) Barth, W. E.; Lawton, R. G. *J. Am. Chem. Soc.* **1966**, *88*, 380. (c) Barth, W. E.; Lawton, R. G. *J. Am. Chem. Soc.* **1971**, *93*, 1730.

- (7) Hopf, H. *Classics in Hydrocarbon Chemistry*; Wiley-VCH: Weinheim, 2000; p 331.
- (8) Sieglitz, A.; Schidlo, W. *Chem. Ber.* **1963**, *96*, 1098.
- (9) (a) Brown, R. F. C.; Harrington, K. J.; McMullen, G. L. *J. Chem. Soc., Chem. Commun.* **1974**, 123. (b) Brown, R. F. C.; Eastwood, F. W.; Jackman, G. P. *Aust. J. Chem.* **1977**, *30*, 1757. (c) Brown, R. F. C.; Eastwood, F. W.; Jackman, G. P. *Aust. J. Chem.* **1978**, *31*, 579. (d) Brown, R. F. C.; Eastwood, F. W.; Harrington, K. J.; McMullen, G. L. *Aust. J. Chem.* **1974**, *27*, 2393.
- (10) (a) Scott, L. T.; Hashemi, M. M.; Meyer, D. T.; Warren, H. B. *J. Am. Chem. Soc.* **1991**, *113*, 7082. (b) Knölker, H.-J.; Braier, A.; Bröcher, D. J.; Jones, P. G.; Piotrowski, H. *Tetrahedron Lett.* **1999**, *40*, 8075. (c) Liu, C. Z.; Rabideau, P. W. *Tetrahedron Lett.* **1996**, *37*, 3437. (d) Cheng, P.-C. M.S. Thesis, University of Nevada, Reno, NV, 1992. (e) Scott, L. T.; Cheng, P.-C.; Hashemi, M. M.; Bratcher, M. S.; Meyer, D. T.; Warren, H. B. *J. Am. Chem. Soc.* **1997**, *119*, 10963. (f) Scott, L. T.; Hashemi, M. M.; Bratcher, M. S. *J. Am. Chem. Soc.* **1992**, *114*, 1920. (g) Borchardt, A.; Fuchicello, A.; Kilway, K. V.; Baldrige, K. K.; Siegel, J. S. *J. Am. Chem. Soc.* **1992**, *114*, 1921.
- (11) Zimmermann, G.; Nuechter, T.; Hagen, S.; Nuechter, M. *Tetrahedron Lett.* **1994**, *35*, 4747.
- (12) Mehta, G.; Panda, G. *Tetrahedron Lett.* **1997**, *38*, 2145.
- (13) Reisch, H. A.; Bratcher, M. S.; Scott, L. T. *Org. Lett.* **2000**, *2*, 1427.
- (14) Seiders, T. J.; Baldrige, K. K.; Siegel, J. S. *J. Am. Chem. Soc.* **1996**, *118*, 2754.
- (15) Sygula, A.; Rabideau, P. W. *J. Am. Chem. Soc.* **1999**, *121*, 7800.
- (16) Seiders, T. J.; Elliott, E. L.; Grube, G. H.; Siegel, J. S. *J. Am. Chem. Soc.* **1999**, *121*, 7804.
- (17) (a) Sygula, A.; Rabideau, P. W. *J. Am. Chem. Soc.* **2000**, *122*, 6323. (b) Xu, G.; Sygula, A.; Marcinow, Z.; Rabideau, P. W. *Tetrahedron Lett.* **2000**, *41*, 9931. (c) Sygula, A.; Xu, G.; Marcinow, Z.; Rabideau, P. W. *Tetrahedron* **2001**, *57*, 3637.
- (18) Maag, R. Diplomarbeit, University of Zurich, Zurich, 2006.
- (19) Marcinow, Z.; Grove, D. I.; Rabideau, P. W. *J. Org. Chem.* **2002**, *67*, 3537.
- (20) Wu, Y.-T.; Hayama, T.; Baldrige, K. K.; Linden, A.; Siegel, J. S. *J. Am. Chem. Soc.* **2006**, *128*, 6870.
- (21) Olah, G. A.; Prakash, G. K. S. *Synthesis* **1976**, 607.
- (22) Sygula, A.; Karlen, S. D.; Sygula, R.; Rabideau, P. W. *Org. Lett.* **2002**, *4*, 3135.
- (23) (a) Semmelhack, M. F.; Helquist, P. M.; Jones, L. D. *J. Am. Chem. Soc.* **1971**, *93*, 5908. (b) Semmelhack, M. F.; Ryono, L. S. *J. Am. Chem. Soc.* **1975**, *97*, 3873. (c) Kende, A. S.; Liebeskind, L. S.; Braitsch, D. M. *Tetrahedron Lett.* **1975**, 3375. (d) Zembayashi, M.; Tamao, K.; Yoshida, J.; Kumada, M. *Tetrahedron Lett.* **1977**, 4089. (e) Tsou, T. T.; Kochi, J. K. *J. Am. Chem. Soc.* **1979**, *101*, 7547. (f) Semmelhack, M. F.; Helquist, P.; Jones, L. D.; Keller, L.; Mendelson, L.; Ryono, L. S.; Smith, J. G.; Stauffer, R. D. *J. Am. Chem. Soc.* **1981**, *103*, 6460. (g) Colon, I.; Kelsey, D. R. *J. Org. Chem.* **1986**, *51*, 2627. (h) Stanger, A.; Ashkenazi, N.; Shachter, A.; Bläser, D.; Stellberg, P.; Boese, R. *J. Org. Chem.* **1996**, *61*, 2549. (i) Stanger, A.; Ashkenazi, N.; Boese, R. J.; Bläser, D.; Stellberg, P. *Chem. Eur. J.* **1997**, *3*, 208. (j) Reisch, H. A.; Enkelmann, V.; Scherf, U. *J. Org. Chem.* **1999**, *64*, 655. (k) Massicot, F.; Schneider, R.; Fort, Y. *J. Chem. Res. (S)* **1999**, 664.
- (24) (a) Yamamoto, T.; Wakabayashi, S.; Osakada, K. *J. Organomet. Chem.* **1992**, *428*, 223. (b) Stanger, A.; Shachter, A.; Boese, R. *Tetrahedron* **1998**, *54*, 1207.
- (25) Sygula, A.; Sygula, R.; Fronczek, F. R.; Rabideau, P. W. *J. Org. Chem.* **2002**, *67*, 6487.
- (26) Cheng, P.-C. Ph.D. Dissertation, Boston College: Boston, MA, 1996; p 212.
- (27) Jones, C. S.; Bandera, D.; Siegel, J. S. Submitted for publication.
- (28) Jones, C. S.; Elliott, E.; Siegel, J. S. *Synlett* **2004**, 187.
- (29) Sygula, A.; Sygula, R.; Rabideau, P. W. *Org. Lett.* **2005**, *7*, 4999.
- (30) Preda, D. V.; Scott, L. T. *Tetrahedron Lett.* **2000**, *41*, 9633.
- (31) Seiders, T. J.; Baldrige, K. K.; Grube, G. H.; Siegel, J. S. *J. Am. Chem. Soc.* **2001**, *123*, 517.
- (32) Hanson, J. C.; Nordman, C. E. *Acta. Crystallogr., Sect. B* **1976**, *B32*, 1147.
- (33) Fedurco, M.; Olmstead, M. M.; Fawcett, W. R. *Inorg. Chem.* **1995**, *34*, 390.
- (34) (a) Haddon, R. C.; Scott, L. T. *Pure Appl. Chem.* **1986**, *58*, 137. (b) Haddon, R. C. *Acc. Chem. Res.* **1988**, *21*, 243. (c) Haddon, R. C. *J. Am. Chem. Soc.* **1990**, *112*, 3385. (d) Haddon, R. C. *Science* **1993**, *261*, 1545.
- (35) Sygula, A.; Abdourazak, A. H.; Rabideau, P. W. *J. Am. Chem. Soc.* **1996**, *118*, 339.
- (36) Seiders, T. J.; Baldrige, K. K.; Elliott, E. L.; Grube, G. H.; Siegel, J. S. *J. Am. Chem. Soc.* **1999**, *121*, 7439.
- (37) Ayalon, A.; Rabinovitz, M.; Cheng, P.-C.; Scott, L. T. *Angew. Chem., Int. Ed. Engl.* **1992**, *31*, 1636.
- (38) Ayalon, A.; Sygula, A.; Cheng, P. C.; Rabinovitz, M.; Rabideau, P. W.; Scott, L. T. *Science* **1994**, *265*, 1065.
- (39) Morita, Y.; Nishida, S.; Kobayashi, T.; Fukui, K.; Sato, K.; Shiomi, D.; Takui, T.; Nakasuji, K. *Org. Lett.* **2004**, *6*, 1397.
- (40) Huang, R.; Huang, W.; Wang, Y.; Tang, Z.; Zheng, L. *J. Am. Chem. Soc.* **1997**, *119*, 5954.
- (41) Scott, L. T. *Pure Appl. Chem.* **1996**, *68*, 291.
- (42) Grube, G. H.; Elliott, E. L.; Steffens, R. J.; Jones, C. S.; Baldrige, K. K.; Siegel, J. S. *Org. Lett.* **2003**, *5*, 713.
- (43) Grasa, G. A.; Nolan, S. P. *Org. Lett.* **2001**, *3*, 119.
- (44) Mizyed, S.; Georghiou, P. E.; Bancu, M.; Cuadra, B.; Rai, A. K.; Cheng, P.; Scott, L. T. *J. Am. Chem. Soc.* **2001**, *123*, 12770.
- (45) Buncel, E.; Crampton, M. R.; Strauss, T. J.; Terrier, F. *Electron Deficient Aromatic and Heteroaromatic-Base Interactions*; Elsevier: New York, 1984.
- (46) Eberhard, M. R.; Wang, Z.; Jensen, C. M. *Chem. Commun.* **2002**, 818.
- (47) Bancu, M.; Rai, A. K.; Cheng, P.-C.; Gilardi, R. D.; Scott, L. T. *Synlett* **2004**, 173.
- (48) For a detailed study about the correlations between the isotopic effect and bowl-to-bowl inversion energy in **67c**, see: Hayama, T.; Siegel, J. S.; et al. Manuscript in preparation. Hayama, T. Diplomarbeit, University of Zurich, Zurich, 2005.
- (49) Georghiou, P. E.; Tran, A. H.; Mizyed, S.; Bancu, M.; Scott, L. T. *J. Org. Chem.* **2005**, *70*, 6158.
- (50) Abdourazak, A. H.; Sygula, A.; Rabideau, P. W. *J. Am. Chem. Soc.* **1993**, *115*, 3010.
- (51) Sygula, A.; Folsom, H. E.; Sygula, R.; Abdourazak, A. H.; Marcinow, Z.; Fronczek, F. R.; Rabideau, P. W. *J. Chem. Soc., Chem. Commun.* **1994**, 2571.
- (52) Sygula, A.; Rabideau, P. W. *J. Chem. Soc., Chem. Commun.* **1994**, 1497.
- (53) Steffens, R. J.; Baldrige, K. K.; Siegel, J. S. *Helv. Chim. Acta* **2000**, *83*, 2644.
- (54) (a) Maggini, M.; Scorrano, G.; Prato, M. *J. Am. Chem. Soc.* **1993**, *115*, 9798. (b) Prato, M.; Maggini, M. *Acc. Chem. Res.* **1998**, *31*, 519.
- (55) Aprahamian, I.; Preda, D. V.; Bancu, M.; Belanger, A. P.; Sheradsky, T.; Scott, L. T.; Rabinovitz, M. *J. Org. Chem.* **2006**, *71*, 290.
- (56) (a) Bratcher, M. S. Ph.D. Dissertation, Boston College, Boston, MA, 1996. (b) Mehta, G.; Srirama Sarma, P. V. V. *Chem. Commun.* **2000**, 19.
- (57) Wu, Y.-T.; Linden, A.; Siegel, J. S. *Org. Lett.* **2005**, *7*, 4353.
- (58) Marcinow, Z.; Sygula, A.; Ellern, A.; Rabideau, P. W. *Org. Lett.* **2001**, *3*, 3527.
- (59) This synthetic method is based on de Meijere's protocol, see: (a) Reiser, O.; Koenig, B.; Meerholz, K.; Heinze, J.; Wellauer, T.; Gerson, F.; Frim, R.; Rabinovitz, M.; de Meijere, A. *J. Am. Chem. Soc.* **1993**, *115*, 3511. (b) Lansky, A.; Reiser, O.; de Meijere, A. *Synlett* **1990**, 405.
- (60) Wegner, H. A.; Scott, L. T.; de Meijere, A. *J. Org. Chem.* **2003**, *68*, 883.
- (61) Aprahamian, I.; Hoffman, R. E.; Sheradsky, T.; Preda, D. V.; Bancu, M.; Scott, L. T.; Rabinovitz, M. *Angew. Chem., Int. Ed.* **2002**, *41*, 1712.
- (62) Seiders, T. J.; Baldrige, K. K.; Siegel, J. S. *Tetrahedron* **2001**, *57*, 3737.
- (63) Sygula, A.; Sygula, R.; Ellern, A.; Rabideau, P. W. *Org. Lett.* **2003**, *5*, 2595.
- (64) Wang, L.; Shevlin, P. B. *Tetrahedron Lett.* **2000**, *41*, 285.
- (65) Wang, L.; Shevlin, P. B. *Org. Lett.* **2000**, *2*, 3703.
- (66) Sygula, A.; Marcinow, Z.; Fronczek, F. R.; Guzei, I.; Rabideau, P. W. *Chem. Commun.* **2000**, 2439.
- (67) Seiders, T. J.; Baldrige, K. K.; O'Connor, J. M.; Siegel, J. S. *J. Am. Chem. Soc.* **1997**, *119*, 4781.
- (68) (a) Fagan, P. J.; Ward, M. D.; Calabrese, J. C. *J. Am. Chem. Soc.* **1989**, *111*, 1698. (b) Ward, M. D.; Fagan, P. J.; Calabrese, J. C.; Johnson, D. C. *J. Am. Chem. Soc.* **1989**, *111*, 1719.
- (69) (a) Dembek, A. A.; Fagan, P. J. *Organometallics* **1995**, *14*, 3741. (b) Dembek, A. A.; Fagan, P. J. *Organometallics* **1996**, *15*, 1319.
- (70) Alvarez, C. M.; Angelici, R. J.; Sygula, A.; Sygula, R.; Rabideau, P. W. *Organometallics* **2003**, *22*, 624.
- (71) Siegel, J. S.; Baldrige, K. K.; Linden, A.; Dorta, R. *J. Am. Chem. Soc.* **2006**, *128*, 10644.
- (72) Vecchi, P. A.; Alvarez, C. M.; Ellern, A.; Angelici, R. J.; Sygula, A.; Sygula, R.; Rabideau, P. W. *Organometallics* **2005**, *24*, 4543.
- (73) Stoddart, M.; Brownie, J. H.; Baird, M. C.; Schmider, H. L. *J. Organomet. Chem.* **2005**, *690*, 3440.
- (74) Vecchi, P. A.; Alvarez, C. M.; Ellern, A.; Angelici, R. J.; Sygula, A.; Sygula, R.; Rabideau, P. W. *Angew. Chem., Int. Ed.* **2004**, *43*, 4497.
- (75) Seiders, T. J.; Baldrige, K. K.; O'Connor, J. M.; Siegel, J. S. *Chem. Comm.* **2004**, 950.

- (76) Petrukhina, M. A.; Andreini, K. W.; Mack, J.; Scott, L. T. *Angew. Chem., Int. Ed.* **2003**, *42*, 3375.
- (77) Petrukhina, M. A.; Andreini, K. W.; Tsefrikas, V. M.; Scott, L. T. *Organometallics* **2005**, *24*, 1394.
- (78) Elliott, E. L.; Hernández, G. A.; Linden, A.; Siegel, J. S. *Org. Biomol. Chem.* **2005**, *3*, 407.
- (79) Kamenno, Y.; Ikeda, A.; Nakao, Y.; Sato, H.; Sakaki, S. *J. Phys. Chem. A* **2005**, *109*, 8055.
- (80) Lee, H. B.; Sharp, P. R. *Organometallics* **2005**, *24*, 4875.
- (81) Caraiman, D.; Koyanagi, G. K.; Scott, L. T.; Preda, D. V.; Bohme, D. K. *J. Am. Chem. Soc.* **2001**, *123*, 8573.
- (82) Kandalam, A. K.; Rao, B. K.; Jena, P. *J. Phys. Chem. A* **2005**, *109*, 9220.
- (83) Ayers, T. M.; Westlake, B. C.; Preda, D. V.; Scott, L. T.; Duncan, M. A. *Organometallics* **2005**, *24*, 4573.
- (84) (a) Meyer, F.; Khan, F. A.; Armentrout, P. B. *J. Am. Chem. Soc.* **1995**, *117*, 9740. (b) Jaeger, T. D.; van Heijnsbergen, D.; Klippenstein, S. J.; von Helden, G.; Meijer, G.; Duncan, M. A. *J. Am. Chem. Soc.* **2004**, *126*, 10981.
- (85) Lewis, K. E.; Smith, G. P. *J. Am. Chem. Soc.* **1984**, *106*, 4650.
- (86) (a) Mehta, G.; Shahk, S. R.; Ravikumarc, K. *J. Chem. Soc., Chem. Commun.* **1993**, 1006. (b) Sastry, G. N.; Jemmis, E. D.; Mehta, G.; Shah, S. R. *J. Chem. Soc., Perkin Trans. 2* **1993**, 1867.
- (87) Sakurai, H.; Daiko, T.; Hirao, T. *Science* **2003**, 1878.
- (88) Sakurai, H.; Daiko, T.; Sakane, H.; Amaya, T.; Hirao, T. *J. Am. Chem. Soc.* **2005**, *127*, 11580.
- (89) Forkey, D. M.; Attar, S.; Noll, B. C.; Koerner, R.; Olmstead, M. M.; Balch, A. L. *J. Am. Chem. Soc.* **1997**, *119*, 5766.
- (90) (a) Desiraju, G. R.; Gavezzotti, A. *J. Chem. Soc., Chem. Commun.* **1989**, 621. (b) Hunter, C. A.; Sanders, J. K. M. *J. Am. Chem. Soc.* **1990**, *112*, 5525. (c) Cozzi, F.; Siegel, J. S. *Pure Appl. Chem.* **1995**, *67*, 683. (d) Miller, L. L.; Mann, K. R. *Acc. Chem. Res.* **1996**, *29*, 417.
- (91) There are also some nonplanar hydrocarbon compounds (but whole molecules are not aromatic compounds) that form column structures, see the following. (a) Triphenylamine derivatives: Field, J. E.; Venkataraman, D. *Chem. Mater.* **2002**, *14*, 962. (b) Tribenzotriquinacene derivatives: Kuck, D.; Schuster, A.; Krause, R. A.; Tellenbröcker, J.; Exner, C. P.; Penk, M.; Bögge, H.; Müller, A. *Tetrahedron* **2001**, *57*, 3587. (c) 4,8,12-Trioxa-12c-phospha-4,8,12,12c-tetrahydrodibenzo[*cd,mn*]pyrene: Krebs, F. C.; Larsen, P. S.; Larsen, J.; Jacobsen, C. S.; Boutton, C.; Thorup, N. *J. Am. Chem. Soc.* **1997**, *119*, 1208.
- (92) Petrukhina, M. A.; Andreini, K. W.; Peng, L.; Scott, L. T. *Angew. Chem., Int. Ed.* **2004**, *43*, 5477.
- (93) Bronstein, H. E.; Choi, N.; Scott, L. T. *J. Am. Chem. Soc.* **2002**, *124*, 8870.

CR050554Q